

การพัฒนาฟิล์มเป่าพอลิแลคติกเอซิดโดยการเติมน้ำยาธรรมชาติผ่านกระบวนการ
วัลคาไนเซชันแบบไดนามิกส์โดยใช้เปอร์ออกไซด์เป็นตัวเชื่อมขวาง



บทคัดย่อและแฟ้มข้อมูลฉบับเต็มของวิทยานิพนธ์ตั้งแต่ปีการศึกษา 2554 ที่ให้บริการในคลังปัญญาจุฬาฯ (CUIR)
เป็นแฟ้มข้อมูลของนิสิตเจ้าของวิทยานิพนธ์ ที่ส่งผ่านทางบัณฑิตวิทยาลัย

The abstract and full text of theses from the academic year 2011 in Chulalongkorn University Intellectual Repository (CUIR)
are the thesis authors' files submitted through the University Graduate School.

วิทยานิพนธ์นี้เป็นส่วนหนึ่งของการศึกษาตามหลักสูตรปริญญาวิศวกรรมศาสตรมหาบัณฑิต
สาขาวิชาวิศวกรรมเคมี ภาควิชาวิศวกรรมเคมี
คณะวิศวกรรมศาสตร์ จุฬาลงกรณ์มหาวิทยาลัย
ปีการศึกษา 2558
ลิขสิทธิ์ของจุฬาลงกรณ์มหาวิทยาลัย

Improvement of poly(lactic acid) blown film by incorporation of natural rubber latex
via dynamic vulcanization using peroxide as curing agent

Miss Parichat Pratumpol



A Thesis Submitted in Partial Fulfillment of the Requirements
for the Degree of Master of Engineering Program in Chemical Engineering
Department of Chemical Engineering
Faculty of Engineering
Chulalongkorn University
Academic Year 2015
Copyright of Chulalongkorn University

Thesis Title	Improvement of poly(lactic acid) blown film by incorporation of natural rubber latex via dynamic vulcanization using peroxide as curing agent
By	Miss Parichat Pratumpol
Field of Study	Chemical Engineering
Thesis Advisor	Associate Professor Anongnat Somwangthanaroj, Ph.D.
Thesis Co-Advisor	Assistant Professor Wanchai Lerdwijitjarud, Ph.D.

Accepted by the Faculty of Engineering, Chulalongkorn University in Partial Fulfillment of the Requirements for the Master's Degree

.....Dean of the Faculty of Engineering
(Professor Bundhit Eua-arporn, Ph.D.)

THESIS COMMITTEE

.....Chairman
(Professor Suttichai Assabumrungrat, Ph.D.)

.....Thesis Advisor
(Associate Professor Anongnat Somwangthanaroj, Ph.D.)

.....Thesis Co-Advisor
(Assistant Professor Wanchai Lerdwijitjarud, Ph.D.)

.....Examiner
(Associate Professor Muenduen Phisalaphong, Ph.D.)

.....External Examiner
(Sunan Tiptipakorn, D.Eng.)

ปารีชาติ ประทุมพล : การพัฒนาฟิล์มเป่าพอลิแลคติกเอซิดโดยการเติมน้ำยางธรรมชาติผ่านกระบวนการวัลคาไนเซชันแบบไดนามิกส์โดยใช้เปอร์ออกไซด์เป็นตัวเชื่อมขวาง (Improvement of poly(lactic acid) blown film by incorporation of natural rubber latex via dynamic vulcanization using peroxide as curing agent) อ.ที่ปรึกษาวิทยานิพนธ์หลัก: รศ. ดร. อนงค์นาฏ สมหวังธนโรจน์, อ.ที่ปรึกษาวิทยานิพนธ์ร่วม: ผศ. ดร. วันชัย เลิศวิจิตรจรัส, 79 หน้า.

งานวิจัยนี้มีวัตถุประสงค์เพื่อเพิ่มสมบัติเชิงกลของฟิล์มเป่าพอลิแลคติกเอซิด (PLA) โดยการผสมกับน้ำยางธรรมชาติ (NRL) และเพื่อปรับปรุงการยึดติดระหว่าง PLA และ ยางธรรมชาติ โดยใช้เปอร์ออกไซด์เป็นตัวเชื่อมขวาง ดังนั้นผลกระทบของการเติมน้ำยางธรรมชาติ และไดควิมิวเปอร์ออกไซด์ (DCP) ที่ส่งผลต่อสัณฐานวิทยา สมบัติเชิงความร้อน สมบัติเชิงกล และสมบัติการซึมผ่านไอน้ำและแก๊สออกซิเจนของฟิล์มเป่า PLA จึงถูกศึกษา จากการวิเคราะห์สมบัติเชิงความร้อนได้ยืนยันว่า PLA และยางธรรมชาติมีความไม่เข้ากัน เนื่องจากค่าอุณหภูมิการเปลี่ยนสถานะคล้ายแก้ว (T_g) ของฟิล์ม PLA/NRL ไม่เปลี่ยนแปลง เมื่อเพิ่มปริมาณน้ำยางธรรมชาติ ในการปรับปรุงสมบัติเชิงกลของฟิล์มเป่า PLA/NRL การยึดติดระหว่าง PLA และยางธรรมชาติ ถูกปรับปรุงโดยเติมตัวเชื่อมขวาง DCP เนื่องจาก PLA ที่ผสมน้ำยางธรรมชาติร้อยละ 10 โดยน้ำหนักของเนื้อยาง (PLA/N10) มีค่าสมบัติเชิงกลสูงที่สุด ดังนั้น PLA/N10 จึงถูกเลือกทำให้เกิดการเชื่อมขวางบางส่วนระหว่างสายโซ่หลักของ PLA และยางธรรมชาติ โดยใช้ DCP ผลเชิงสัณฐานวิทยาแสดงให้เห็นว่าการเติม DCP ส่งผลให้โดเมนยางมีขนาดเล็กลงและการเกิดโพรงของฟิล์มลดลง การเกิดปฏิกิริยาการเชื่อมขวางกันระหว่าง PLA และยางธรรมชาติถูกยืนยันจากผลของ FTIR จากผลการทดลองแสดงสมบัติเชิงกลของฟิล์ม PLA/N10/DCP มีค่าความทนต่อแรงดึง ค่าโมดูลัสของยัง ค่าระยะยืด ณ จุดขาด ค่าความเหนียว ค่าความทนต่อแรงกระแทก และค่าความทนต่อแรงฉีกขาดสูงสุด เมื่อเติม DCP ที่ปริมาณ 0.003 ส่วนในร้อยส่วนของระบบ(phr) ดังนั้นฟิล์ม PLA/N10 ผสม DCP ที่ปริมาณ 0.003 phr จึงเป็นองค์ประกอบที่เหมาะสมสำหรับการปรับปรุงการยึดติดของ PLA และยางธรรมชาติ

ภาควิชา วิศวกรรมเคมี

สาขาวิชา วิศวกรรมเคมี

ปีการศึกษา 2558

ลายมือชื่อนิสิต

ลายมือชื่อ อ.ที่ปรึกษาหลัก

ลายมือชื่อ อ.ที่ปรึกษาร่วม

5670281421 : MAJOR CHEMICAL ENGINEERING

KEYWORDS: CROSSLINK REACTION / DICUMYL PEROXIDE(DCP) / MECHANICAL PROPERTIES / NATURAL RUBBER LATEX / POLY(LACTIC ACID) (PLA)

PARICHAT PRATUMPOL: Improvement of poly(lactic acid) blown film by incorporation of natural rubber latex via dynamic vulcanization using peroxide as curing agent. ADVISOR: ASSOC. PROF. ANONGNAT SOMWANGTHANAROJ, Ph.D., CO-ADVISOR: ASST. PROF. WANCHAI LERDWIJITJARUD, Ph.D., 79 pp.

This research aims to enhance the mechanical properties of poly(lactic acid) (PLA) blown film by incorporation of natural rubber latex (NRL) and to improve the interfacial adhesion between PLA and rubber (NR) using peroxide as curing agent. Hence, the effect of the presence of NRL and dicumyl peroxide (DCP) on physical, thermal and mechanical properties as well as water and oxygen permeation of PLA blown films were studied. The thermal analysis strongly confirmed the immiscibility of PLA and NR in which T_g of PLA/NRL films did not change when NRL content increased. In order to improve the mechanical properties of PLA/NRL blown films, the interfacial adhesion between PLA and NR was improved by adding DCP as curing agent. Since PLA blended with 10 wt% natural rubber (PLA/N10) had the highest mechanical properties, PLA/N10 was selected to partially crosslink between PLA main chains and NR by using DCP. The morphological results indicated that the addition of DCP induced smaller domain sized rubber and less cavitation in films. From FTIR results, the crosslink reaction between PLA and NR was confirmed. The results showed that the mechanical properties of PLA/N10/DCP films had the highest tensile strength, Young's modulus, elongation at break, toughness, impact strength and tear strength with an addition of DCP at 0.003 phr. Therefore, PLA/N10 blended with DCP at 0.003 phr was the optimal composition for improving the interfacial adhesion of PLA and NR.

Department:	Chemical Engineering	Student's Signature
Field of Study:	Chemical Engineering	Advisor's Signature
Academic Year:	2015	Co-Advisor's Signature

ACKNOWLEDGEMENTS

I would like to express my sincere thanks to my thesis advisor, Associate Professor Dr. Anongnat Somwangthanaroj and my co-advisor, Assistant Professor Dr. Wanchai Lerdwijitjarud for precious advice, guidance and support throughout my research thesis and editing of this thesis.

I am great appreciate to the chairman, Professor Dr. Suttichai Assabumrungrat, and committee members, Associate Professor Dr. Muenduen Phisalaphong and Dr.Sunan Tiptipakorn who provided significant suggestions and valuable recommendations for this research.

In addition, I am grateful to everyone in the Polymer Engineering Research Laboratory, Department of Chemical Engineering, Chulalongkorn University, for discussion and friendly encouragement and given comments. Furthermore, I would like to thank my friends, Dr. Chutimar Deetuum and Mr. Chavakorn Samthong for their kind helps with editing my thesis and answered my questions all the times.

Finally, I would like to wholeheartedly give all gratitude to the members of my family for their generous encouragement during my entire studies. Also, every person who deserves thanks for the encouragement and support that cannot be listed.

CONTENTS

	Page
THAI ABSTRACT	iv
ENGLISH ABSTRACT	v
ACKNOWLEDGEMENTS	vi
CONTENTS	vii
LIST OF FIGURES	x
LIST OF TABLES	xiii
CHAPTER I INTRODUCTION.....	1
1.1 General introduction.....	1
1.2 Objectives	3
1.3 Scopes of the research	3
CHAPTER II THEORY AND LITERATURE REVIEWS	4
2.1 Incorporation of PLA with different types of natural rubber for blown films packaging	4
2.2 Effect of rubber content on the mechanical properties of the molded specimen	7
2.3 Effect of domain size of rubber on mechanical properties of the molded specimen	8
2.4 Effect of interfacial adhesion on mechanical properties the molded specimen	10
CHAPTER III EXPERIMENTS.....	13
3.1 Materials.....	13
3.2 Preparation of PLA/NRL and PLA/NRL/DCP films	14
3.3 Characterization.....	17

	Page
3.3.2 Morphology	17
3.3.3 Thermal properties.....	18
3.3.5 Mechanical properties	18
3.3.6 Permeability properties	19
3.3.7 Characterization of crosslink reaction of PLA/NRL/DCP films.....	20
3.3.8 Gel content	20
CHAPTER IV RESULTS AND DISCUSSION	22
4.1 Effect of rubber content on the properties of PLA/NRL films.....	25
4.1.1 Morphology.....	25
4.1.2 Thermal properties.....	28
4.1.3 Mechanical properties	30
4.1.4 Gas permeability	36
4.2 Effect of dynamic vulcanization by DCP on the properties of PLA/NRL/DCP films	38
4.2.1 Morphology.....	38
4.2.2 Characterization of crosslink reaction of PLA/NRL/DCP films.....	41
4.2.3 Gel content	43
4.2.4 Thermal properties.....	44
4.2.5 Mechanical properties	47
4.2.6 Gas permeability	52
CHAPTER V CONCLUSIONS AND RECOMMENDATIONS	54
5.1 Conclusions	54
5.2 Recommendations	56

	Page
REFERENCES	57
APPENDICES.....	63
APPENDIX A Thermal properties.....	64
APPENDIX B Mechanical properties.....	66
APPENDIX C Oxygen and water permeation	76
APPENDIX D The size distribution of rubber domain	78
VITA.....	79



LIST OF FIGURES

	Page
Figure 2.1 SEM micrographs of cross-sectional fractured surfaces of PLA blown films of (a) PLA/NRL15 wt% NR (MD), (b) PLA/NRL15 wt% NR (TD), (c) PLA/ADS 15 wt% NR (MD), and (d) PLA/ADS15 wt% NR (TD).....	6
Figure 2.2 SEM images of PLA/35 wt% NR surface after etching with dichloromethane for (a) 1 min and (b) 4 min	8
Figure 2.3 TEM images of the PHBV/PBS (80:20) blends with an addition of DCP content of (a) 0, (b) 0.2, (c) 0.5, and (d) 1.0 phr	9
Figure 2.4 FTIR absorption spectra of individual polymers and residues of extracted PLA/NR/para tertiary butylphenol formaldehyde resin (PP6R4), PLA/NR/sulfur (SP6R4) and PLA/NR/DPC (DP6R4) by dichloromethane	11
Figure 2.5 Reactions of DCP initiating PLA and NR forming macromolecular free radicals (RO• is for cumyloxy radical)	12
Figure 3.1 Chemical structures of (a) polylactic acid (PLA), (b) cis-1,4polyisoprene (NR) and (c) Dicumyl peroxide (DCP).....	13
Figure 3.2 Experimental procedure.....	21
Figure 4.1 The appearance of films for all component a) neat PLA, b) PLA/ADS10.....	24
Figure 4.2 SEM micrograph of cross-sectional fractured surface in MD of a) neat PLA, b) PLA/N10, c) PLA/N20 and d) PLA/N30	26
Figure 4.3 SEM micrograph of cross-sectional fractured surface in TD of a) neat PLA, b) PLA/N10, c) PLA/N20 and d) PLA/N30.....	27

Figure 4.4 DSC thermograms in second heating scan of PLA/NRL blend	29
Figure 4.5 Tensile strength of neat PLA and PLA/NRL films	32
Figure 4.6 Young's modulus of neat PLA and PLA/NRL films	32
Figure 4.7 Elongation at break of neat PLA and PLA/NRL films	33
Figure 4.8 Tensile toughness of neat PLA and PLA/NRL films	33
Figure 4.9 Impact strength of neat PLA and PLA/NRL films.....	34
Figure 4.10 Tear strength of neat PLA and PLA/NRL films.....	34
Figure 4.11 The possible tear mechanisms in PLA/NRL films	35
Figure 4.12 Water permeation of neat PLA and PLA/NRL films	37
Figure 4.13 Oxygen permeation of neat PLA and PLA/NRL films	37
Figure 4.14 Morphology of cross-sectional fractured surfaces of PLA/N10/DCP films in MD at DCP content of a) 0 phr, b) 0.003 phr, c) 0.005 phr and d) 0.01 phr	39
Figure 4.15 Morphology of surfaces of PLA/N10/DCP films at DCP content of a) 0 phr, b) 0.003 phr, c) 0.005 phr and d) 0.01 phr	40
Figure 4.16 FTIR absorption spectra of neat PLA, NRL and residual of dichloromethane-extracted PLA/N10/DCP at DCP content of 0.003, 0.005 and 0.01 phr	42
Figure 4.17 DSC thermograms in the second heating scan of PLA/N10/DCP blends	45
Figure 4.18 Tensile strength of PLA/N10 with DCP content of 0.003, 0.005 and 0.01 phr	49
Figure 4.19 Young's modulus of PLA/N10 with DCP content of 0.003, 0.005 and 0.01 phr	49

Figure 4.20 Elongation at break of PLA/N10 with DCP content of 0.003, 0.005 and 0.01 phr.....	50
Figure 4.21 Tensile toughness of PLA/N10 with DCP content of 0.003, 0.005 and 0.01 phr.....	50
Figure 4.22 Impact strength of PLA/N10 with DCP content of 0.003, 0.005 and 0.01 phr.....	51
Figure 4.23 Tear strength of PLA/N10 with DCP content of 0.003, 0.005 and 0.01 phr.....	51
Figure 4.24 Water vapor permeation of PLA/N10 with DCP content of 0.003, 0.005 and 0.01 phr.....	53
Figure 4.25 Oxygen permeation of PLA/N10 with DCP content of 0.003, 0.005 and 0.01 phr.....	53
Figure A.1 DSC thermograms in the first heating scan of PLA/NRL films	64
Figure A.2 DSC thermograms in the first heating scan of PLA/N10/DCP films	65
Figure B.1 Stress strain curve of PLA/NRL blend films.....	66
Figure B.2 Stress strain curve of PLA/N10 with DCP content of 0.003, 0.005 and 0.01 phr.....	66
Figure D.1 Size distribution of NR domain in the PLA/N10/DCP films for different DCP content a) 0 phr, b) 0.003 phr, c) 0.005 phr and d) 0.01 phr.....	78

LIST OF TABLES

	Page
Table 3.1 Composition of PLA/NRL and PLA/NRL/DCP sample.....	16
Table 4.1 Thermal properties of PLA/NRL blends in the second heating scan	30
Table 4.2 Number average diameter (D_n), volume average diameter (D_v) and polydispersity (PD) of PLA/N10/DCP films at different DCP contents.....	40
Table 4.3 The ratio of absorption peak area (APLA/ANR) of the residual of PLA/N10/DCP films at different DCP contents	43
Table 4.4 Gel content of PLA/N10/DCP films at different DCP contents	44
Table 4.5 Thermal properties of PLA/N10/DCP blends in the second heating scan	46
Table A.1 Thermal properties of PLA/NRL films in the first heating scan	64
Table A.2 Thermal properties of PLA/NRL films in the first heating scan	65
Table B.1 Tensile properties in MD of PLA films.....	66
Table B.2 Tensile properties in MD of PLA/N10 films	67
Table B.3 Tensile properties in MD of PLA/N20 films.....	68
Table B.4 Tensile properties in MD of PLA/N30 films.....	68
Table B.5 Tensile properties in MD of PLA/N10 films blended with 0.003 phr of DCP.....	69
Table B.6 Tensile properties in MD of PLA/N10 films blended with 0.005 phr of DCP.....	69

Table B.7 Tensile properties in MD of PLA/N10 films blended with 0.01 phr of DCP	70
Table B.8 Tensile properties in TD of Neat PLA films.....	70
Table B.9 Tensile properties in TD of PLA/N10 films.....	71
Table B.10 Tensile properties in TD of PLA/N20 films.....	71
Table B.11 Tensile properties in TD of PLA/N30 films.....	72
Table B.12 Tensile properties in TD of PLA/N10 films blended with 0.003 phr of DCP.....	72
Table B.13 Tensile properties in TD of PLA/N10 films blended with 0.005 phr of DCP.....	73
Table B.14 Tensile properties in TD of PLA/N10 films blended with 0.01 phr of DCP.....	73
Table B.15 Impact strength of PLA/NRL films.....	74
Table B.16 Impact strength of PLA/N10/DCP.....	74
Table B.17 Tear strength of PLA/NRL	75
Table B.18 Tear strength of PLA/N10/DCP	75
Table C.1 Water permeation of PLA/NRL films	76
Table C.2 Water permeation of PLA/N10/DCP films	76
Table C.3 Oxygen permeation of PLA/NRL films	77
Table C.4 Oxygen permeation of PLA/N10/DCP films	77

CHAPTER I

INTRODUCTION

1.1 General introduction

Currently, most of plastic packagings have been made from the nonrenewable petroleum resources. Concerning about the environmental impacts such as global warming, biodegradable thermoplastics such as polycaprolactone (PCL), poly(butylene succinate) (PBS), poly(butylene adipate)-co-terephthalate (PBAT) and poly(lactic acid) (PLA) have been intensively studied. Among them, PLA is a promising alternative bioplastic due to its high strength, excellent transparency and biodegradability [1, 2]. However, PLA is brittle and has low gas permeation. According to previous literatures, these drawbacks can be solved by blending PLA with air dried sheet natural rubber (ADS) [3-5]. Toughness and gas permeation of modified PLA/ADS blown films were higher than those of neat PLA. Nevertheless, the surface of PLA/ADS films was not smooth due to large domain size of rubber in the PLA matrix as a result of particle agglomeration [3]. PLA blended with natural rubber latex (NRL) consisting of 40 wt% of water and 60 wt% of dried natural rubber (NR) content gave a smoother film surface that is suitable for food packaging applications [6]. Moreover, small domain sized NR in PLA matrix was beneficial the toughening of PLA [7]. Nonetheless, the maximum NR

content in PLA/NRL films was limited to only 15 wt% owing to the processing limitations [6]. Therefore, this research would find the blending process of PLA at higher NRL content. However, PLA and NR domains were immiscible [8], contributing to poor compatibility and weak interfacial adhesion; thus, increasing NR content led to lower mechanical properties, especially toughness.

It was found that crosslinked binary blend polymer via dynamic vulcanization method by using peroxide as curing agent resulted in a reduction of domain size in polymer matrix due to the enhancement of interfacial adhesion between phases [9]. Herein, dicumyl peroxide (DCP) as commercial cross-linker was added to enhance the compatibility between PLA and NR domains.

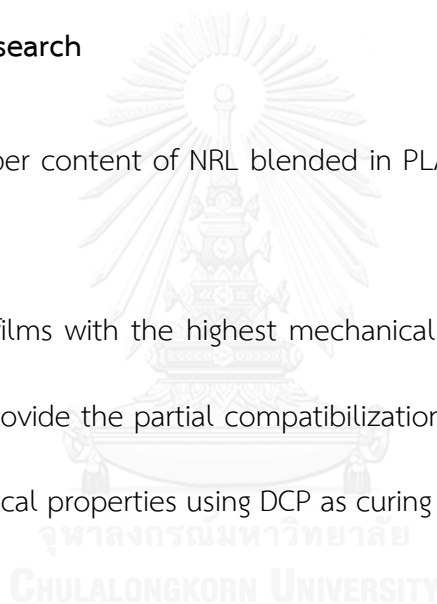
This research focused on studying the effect of NRL content on the properties of PLA/NRL films. Blending PLA and NRL at different DCP content was also investigated. Thermal and mechanical properties as well as morphology and gas permeation of films was measured. The crosslink reaction of crosslinked PLA/NRL via dynamic vulcanization was also considered.

1.2 Objectives

1. To study the effect of dried rubber content in NRL on the properties of PLA/NRL blown films
2. To investigate the effect of content of DCP as curing agent on the properties of PLA/NRL/DCP blown films

1.3 Scopes of the research

1. The dried rubber content of NRL blended in PLA/NRL will be varied at 10, 20 and 30 wt%.
2. The PLA/NRL films with the highest mechanical properties from the first part will be selected to provide the partial compatibilization between PLA and NR and to enhance the mechanical properties using DCP as curing agent at 0.003, 0.005 and 0.01 phr.



CHAPTER II

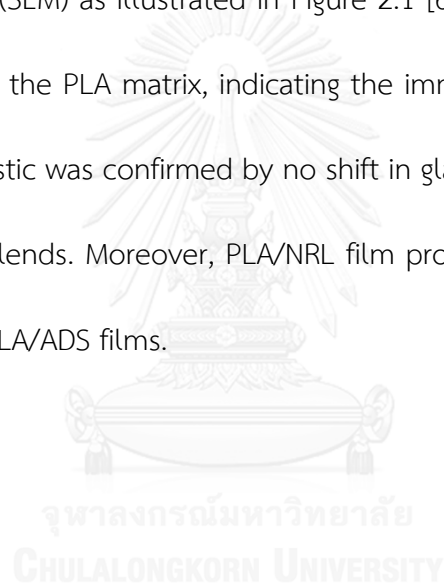
THEORY AND LITERATURE REVIEWS

2.1 Incorporation of PLA with different types of natural rubber for blown films packaging

Neat poly(lactic acid) (PLA) blown films are brittle and have poor mechanical properties which are not suitable to be used as packaging; therefore, the materials having high elasticity and high impact strength material such as natural rubber (NR) were incorporated. More importantly, using NR not only improved the properties of films, but also reduced the cost of packaging and maintained the environmentally friendly properties of PLA/NR. According to the previous work, the tensile toughness of neat PLA (35.43 mJ) was improved by blending with 20 wt% air dried sheet rubber (ADS) (69.52 mJ) and 20 wt% standard Thai rubber grade 5L (STR5L) (273.34 mJ) [3]. Moreover, PLA blended with masticated STR5L gave smoother film surface than PLA blended with masticated ADS. STR5L had high thermal sensitivity than ADS and the molecular weight and viscosity of STR5L were easily reduced, leading to the formation of small sized NR domains.

PLA was also blended with natural rubber latex (NRL) (60% dried rubber content) using a twin screw extruder. However, the maximum loading of NR in NRL was limited

to only 15 wt% because NRL contained high water content, resulting in an overflow of NRL at the hopper feeder of the extruder. The elongation at break of the PLA/NRL films was reached the maximum value at 12.5 wt% NR. Further increasing NRL to 15 wt% NR reduced the elongation at break and gas permeation, which might be due to the fact that the total NR content cannot be fed into the hopper. The morphologies of blends of PLA/15 wt% NR in NRL and PLA/15 wt% ADS were observed by a scanning electron microscope (SEM) as illustrated in Figure 2.1 [6]. It showed many debonded rubber domains from the PLA matrix, indicating the immiscibility of PLA and NR. The immiscible characteristic was confirmed by no shift in glass transition temperature (T_g) [3-5, 10] of PLA/NR blends. Moreover, PLA/NRL film provided constant thickness and smoother film than PLA/ADS films.



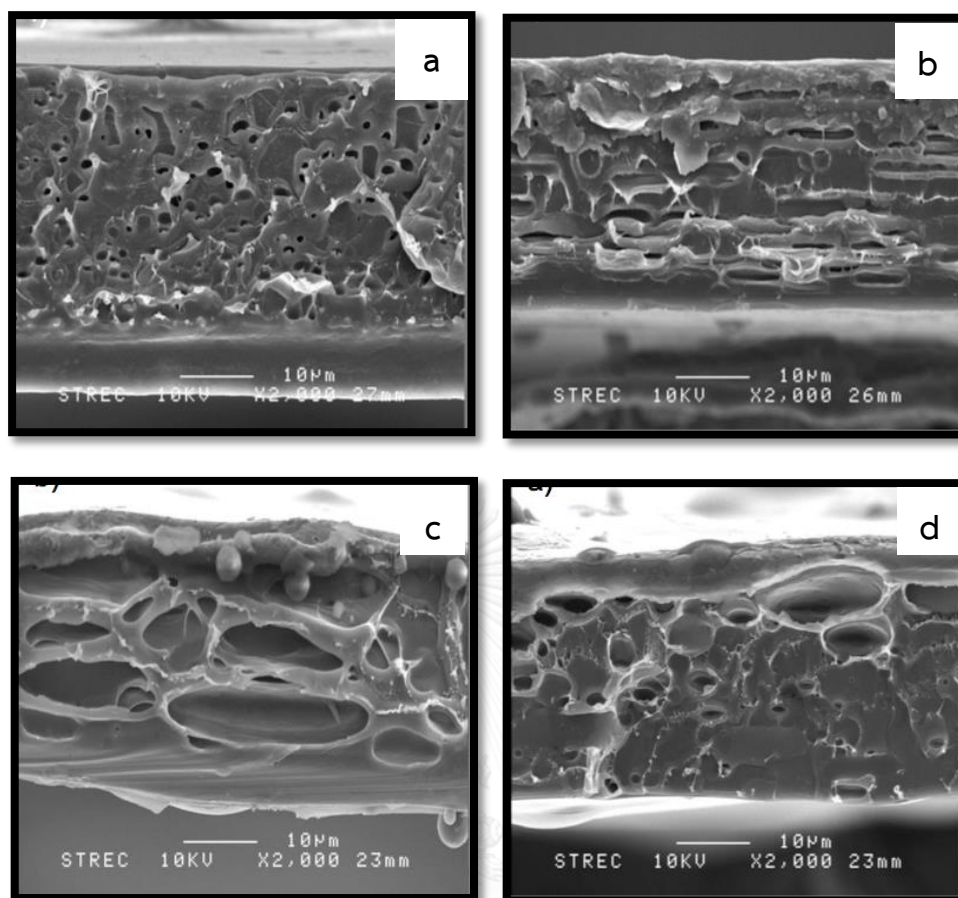


Figure 2.1 SEM micrographs of cross-sectional fractured surfaces of PLA blown films of (a) PLA/NRL15 wt% NR (MD), (b) PLA/NRL15 wt% NR (TD), (c) PLA/ADS 15 wt% NR

(MD), and (d) PLA/ADS15 wt% NR (TD) [6]

2.2 Effect of rubber content on the mechanical properties of the molded specimen

Rubber content is the important factor influencing the mechanical properties of the polymer blends. The elongation at break and toughness of polymer blends increased as increasing rubber content because of the elasticity of rubber. When rubber was added over the optimum value in the polymer matrix, the mechanical properties of specimen would drastically reduce due to the coalescence of NR droplet, leading to larger NR domain size, and the phase separation between PLA and NR [11]. The compression molded specimen of PLA blended with 10 wt% NR showed an increase in elongation at break from 5% (neat PLA) to 200% and a decrease in elongation at break to 70% with 20 wt% rubber content [12]. However, the elongation at break of the injection molded specimen of PLA blended with 10 wt% NR was only 10% due to larger rubber domain than those of compression molded specimen [13]. On the other hand, the injection molded specimen of PLA blended with 35 wt% NR exhibited the enhanced impact strength of 500 J/m, approximately 7 folds of that of neat PLA. The SEM images of the surfaces of PLA/35 wt% NR after etching with dichloromethane to remove PLA phase are illustrated in Figure 2.2. It is observed that the co-continuous structure of NR phase after removing PLA is the reason for the enhancement of impact strength in PLA/NR blends.

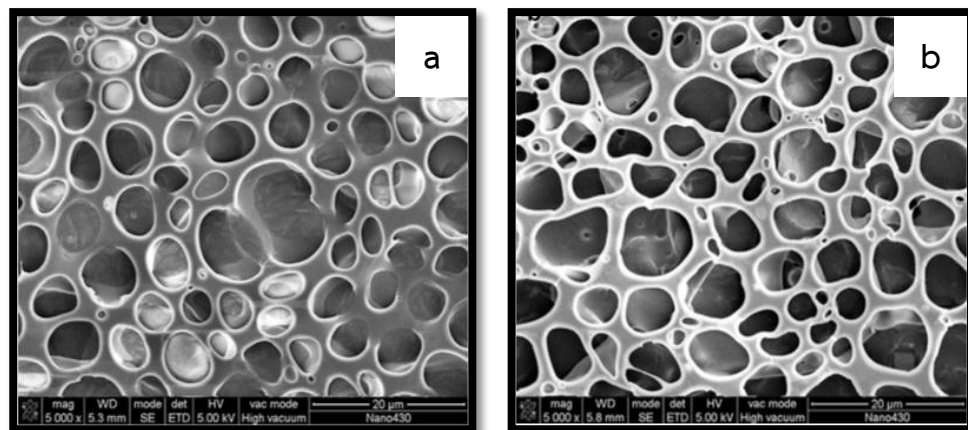


Figure 2.2 SEM images of PLA/35 wt% NR surface after etching with dichloromethane for (a) 1 min and (b) 4 min [13]

2.3 Effect of domain size of rubber on mechanical properties of the molded specimen

NR domain acts as stress concentrator, initiating the crazes, cracks and propagation during fracture process. Crazing induced dissipation energy in the polymer matrix that retards those of crack and propagation phenomenon [5], leading to increased toughness of PLA. The small domain size is more effective to enhance toughness of PLA because the total surface area of small domain sized NR is higher than that of the larger one. Poor compatibility between two polymers resulted in relatively large particle size of dispersed phase owing to weak interfacial adhesion. The effect of addition of dicumyl peroxide (DCP) on the morphology of poly(β -hydroxybutyrate)-co-(β -hydroxyvalerate) (PHBV) blended with poly(butylene succinate) (PBS) revealed that

the size of PBS domains decreased as increasing DCP content [9], as can be seen in TEM image in Figure 2.3. The in situ compatibilization of PHBV/PBS at the weight ratio of 80/20 with 0.5 phr of DCP showed an increase in elongation at break from 8% (without any addition of DCP) to 400%.

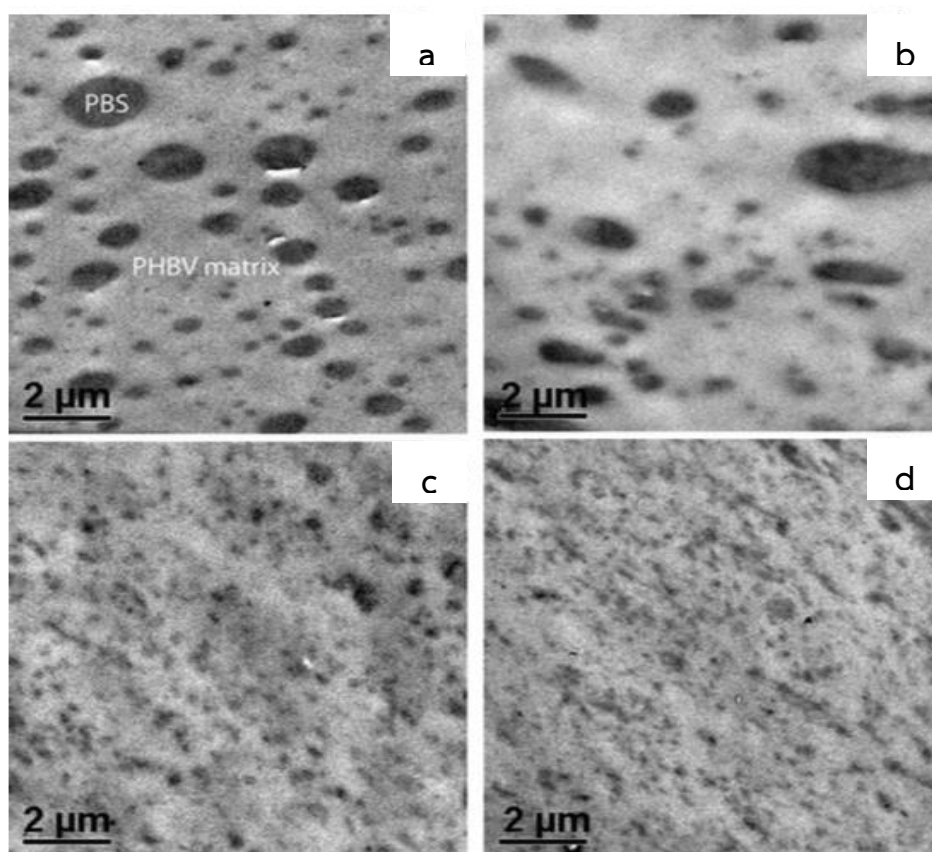


Figure 2.3 TEM images of the PHBV/PBS (80:20) blends with an addition of DCP content of (a) 0, (b) 0.2, (c) 0.5, and (d) 1.0 phr [9]

2.4 Effect of interfacial adhesion on mechanical properties the molded specimen

It was found that an incorporation of NR significantly improved the mechanical properties of PLA blown film. However, the difference in polarity of polymers may result in poor interfacial adhesion between PLA matrix and NR domains [7, 8, 10]. To improve the toughness, impact strength, and elongation at break, the interfacial interaction between two phases should be modified.

Dynamic vulcanization is a selective vulcanization of the rubber phase upon intensively the mixing or kneading the rubber with the molten thermoplastic polymer with the presence of curing agent so the final product is called thermo plastic vulcanizate (TPV) [14]. The commercial curing agent is divided into 3 systems: sulfur, peroxide and other systems. Yuan et al. found that PLA/NR blends modified via dynamic vulcanization using dicumyl peroxide (DCP), sulfur and para tertiary butylphenol formaldehyde resin as curing agents revealed the crosslink reaction between PLA chains and NR domains [1]. The crosslink reaction led to an improved interfacial adhesion between PLA matrix and NR domains. FTIR spectra of the vulcanized blends are illustrated in Figure 2.4. The absorption peak at 1750 cm^{-1} represents the stretching of carbonyl group of PLA. The sample extracted by dichloromethane (good solvent for PLA) was closely identical to those of pure NR, suggesting that free PLA was removed completely. Nonetheless, the absorption peak

at 1757 cm^{-1} was visible for all samples, confirming that PLA crosslinked with NR via dynamic vulcanization method.

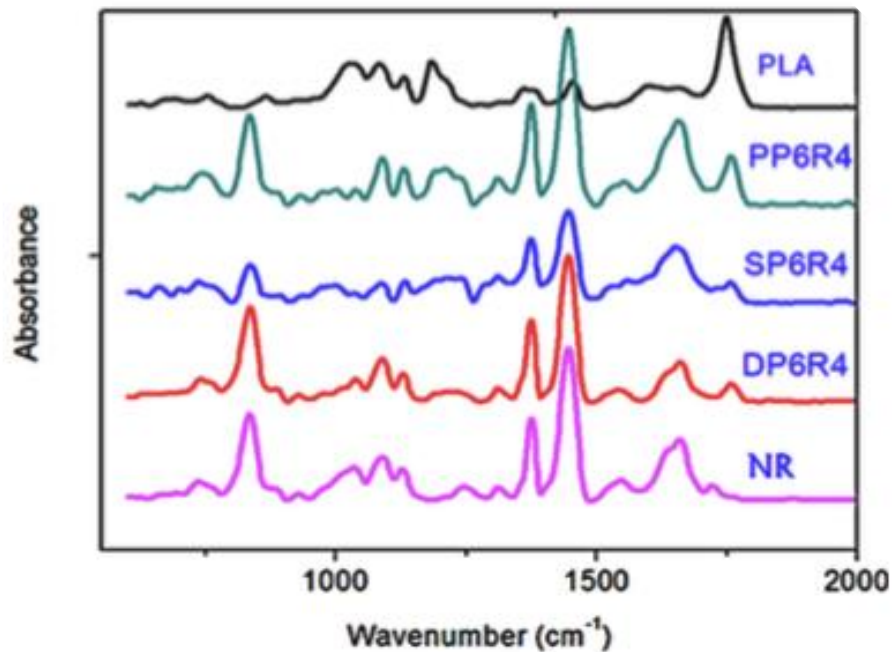


Figure 2.4 FTIR absorption spectra of individual polymers and residues of extracted PLA/NR/para tertiary butylphenol formaldehyde resin (PP6R4), PLA/NR/sulfur (SP6R4) and PLA/NR/DPC (DP6R4) by dichloromethane [1]

The mechanical properties of PLA/NR blends were improved by adding 1.5 wt% of dicumyl peroxide (DCP). The Izod impact strength of PLA blended with 20 wt% NR was 5.1 kJ/m^2 , whereas Izod impact strength of vulcanized PLA/NR/DCP blend was increased to 7.5 kJ/m^2 . Further, the Izod impact strength of PLA/NR/DCP blend was increased to 58.3 kJ/m^2 , approximately 21 times higher than that of neat PLA (2.75 kJ/m^2), and maximum elongation at break of 200% at 35 wt% NR loading. The

mechanical properties of PLA/NR/DCP blend were increased due to the enhanced interfacial interaction as evidenced by no debonding or voids between PLA and NR phase [15]. However, further increasing DCP loading resulted in a reduction in elongation at break because highly crosslinked rubber hinders the deformation of specimens [16]. The possible crosslink reaction between PLA and NR by using DCP as curing agent is shown in Figure 2.5. DCP produces free radicals ($RO\bullet$) which can abstract hydrogen from PLA main chain and subsequently lead to the formation of reactive site of PLA. The NR chains also leave the active site from abstraction of hydrogen bond or addition of DCP radical. Then, the free radicals will be coupled, resulting in crosslink between PLA and NR, or between NR and NR.

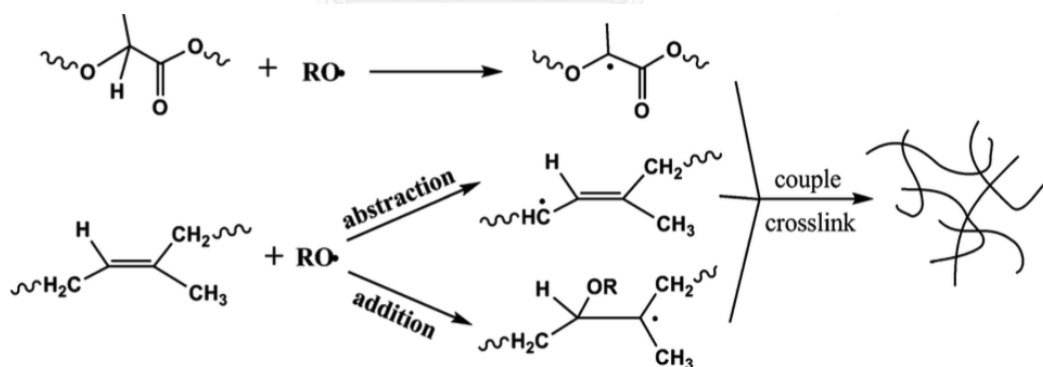


Figure 2.5 Reactions of DCP initiating PLA and NR forming macromolecular free radicals ($RO\bullet$ is for cumyloxy radical) [16]

CHAPTER III

EXPERIMENTS

3.1 Materials

PLA 2003D was purchased from NatureWorks, USA. Commercial high ammonia natural rubber latex (NRL) (61.36 % dried rubber content) was purchased from Rubber Research Institute of Thailand, Kasetsart University. Dicumyl peroxide (DCP), which is a curing agent, was supplied by Arkema, Thailand. The chemical structures of PLA, natural rubber (NR) and DCP are illustrated in Figure 3.1.

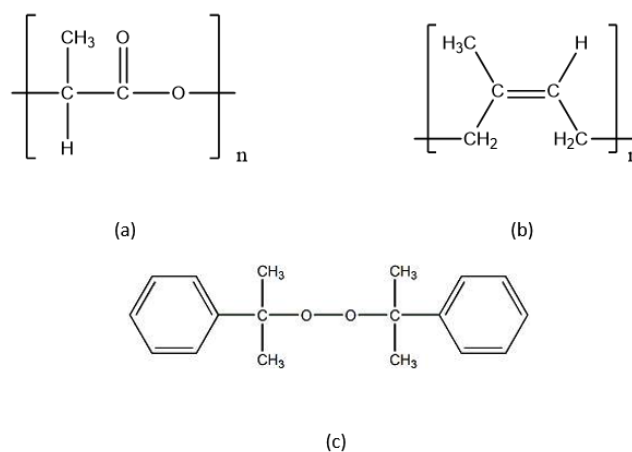


Figure 3.1 Chemical structures of (a) polylactic acid (PLA), (b) cis-1,4polyisoprene (NR) and (c) Dicumyl peroxide (DCP)

3.2 Preparation of PLA/NRL and PLA/NRL/DCP films

NRL was filtered through the cheesecloth before blending with PLA by using a co-rotating twin screw extruder (Labtech Engineering, Thailand, L/D=40 and D=20). The processing temperature was controlled to be in a range of 180-185 °C and a screw speed was 85 rpm. The abbreviations of PLA blended with NRL at 10, 20, and 30 wt% NR are PLA/N10, PLA/N20, and PLA/N30, respectively. Incorporation of high NRL loading (such as 15 wt% NR) in one stage was hardly processed because the latex might overflow at the hopper feeder of the extruder. Therefore, the blending of NRL with PLA pellets was divided into 5 stages by adding 10 wt% NR in each stage. For preparing 1 kg of PLA/N30 pellets, 700 g of PLA was blended with 126.76 g of NRL (77.78 g of NR) (10 wt% NR in the first stage compound). For the second stage, 778.78 g of compound from the first stage was blended with 158.44 g of NRL through the extruder, then the compound from the second stage was obtained (20 wt% NR in second stage compound). For the third stage, 875 g of compound from the second stage was blended with 203.71 g of NRL again achieving 30 wt% NR in PLA/N30 pellets. In order to provide well mixing material, the compound were melt-mixed again in the twin screw extruder without any addition of NRL for additional 2 times (5 times in total). To eliminate the effect of temperature processing and the mixing time, all compound and neat PLA were processed at the same processing conditions.

For the crosslinked films, the DCP content was varied at 0.003, 0.005 and 0.01 gram per hundred gram of PLA/NRL blends (phr). DCP, PLA pellet and NRL were

physically premixed together before blending by using twin screw extruder. The processing condition was the same as the preparation of PLA/NRL. All compositions are illustrated in Table 3.1. In addition, the compounds were dried in an oven at 60 °C for 24 hours and kept in a PE zipped lock plastic bag.

Blown films were obtained by using a single screw extruder ($L/D = 25$, $D = 20$ mm) attached to a blown film die (Collin, Blown film line BL 180/400E, Germany). The processing temperature was set at 190-195 °C and the screw speed was 85 rpm. The blow up ratio was 2.3 and the take-off ratio was 3.5.



Table 3.1 Composition of PLA/NRL and PLA/NRL/DCP sample

Sample	Stages										
	1			2		3		4		5	
	PLA (wt %)	NR (wt %)	DCP (phr)	PLA (wt %)	NR (wt %)	PLA (wt %)	NR (wt %)	PLA (wt %)	NR (wt %)	PLA (wt %)	NR (wt %)
PLA/N10	90	10	-	X		X		X		X	
PLA/N20	90	10	-	80	20	X		X		X	
PLA/N30	90	10	-	80	20	70	30	X		X	
PLA/N10/DCP	90	10	0.003, 0.005 and 0.01	X		X		X		X	

X = Melt Blending without any addition of NRL

3.3 Characterization

3.3.2 Morphology

The morphology in the cross-sectional surface of PLA/NRL and PLA/NRL/DCP blown films in machine direction (MD) and transverse direction (TD) was observed by using a scanning electron microscope (SEM, JEOL JSM 5410 LV). All samples were fractured in liquid nitrogen and stained with osmium tetroxide vapor to increase a contrast between PLA matrix and NR domain. Eventually, the samples were coated with gold layer to prevent electrical discharge prior to SEM observation. The number average diameter (D_n), volume average diameter (D_v) and polydispersity (PD) were determined by image analysis software (ImageJ software, Rasband, W.S., ImageJ, U.S. National Institutes of Health, Bethesda, Maryland, USA). D_n , D_v and PD were defined in equation 5, 6 and 7, respectively [17]. Typically, about 300 domains were analyzed per sample and the average Feret's diameter was calculated.

$$D_n = \frac{\sum N_i D_i}{\sum N_i} \quad (3.1)$$

$$D_v = \frac{\sum N_i D_i^4}{\sum N_i D_i^3} \quad (3.2)$$

$$PD = \frac{D_v}{D_n} \quad (3.3)$$

D_i = diameter of each NR domain

N_i = number of NR domain with diameter

3.3.3 Thermal properties

Thermal properties of PLA/NRL and PLA/NRL/DCP films were investigated by using differential scanning calorimetry (Perkin Elmer, Diamond DSC, USA). The films were cut and weighed approximately 5-10 mg and put in an aluminum pan. The samples were heated from 30 to 200 °C at a heating rate of 10 °C/min under nitrogen atmosphere. Glass transition temperature (T_g), cold crystallization temperature (T_{cc}) and melting temperature (T_m) of the films were collected from the DSC thermogram. The degree of crystallinity ($\%X_c$) was calculated as shown in the following equation.

$$\%X_c = \frac{\Delta H_m - \Delta H_{cc}}{(\Delta H_m^0 \times \Phi)} \times 100 \quad (3.4)$$

where ΔH_m and ΔH_{cc} were the enthalpies of the melting and cold crystallization of PLA/NRL and PLA/NRL/DCP films, respectively. ΔH_m^0 was the melting enthalpy of 100% crystalline PLA (93 J/g) [18]. Φ was weight fraction of PLA matrix in the blends.

3.3.5 Mechanical properties

Tensile strength, Young's modulus, elongation at break and tensile toughness of films in both MD and TD were evaluated according to ASTM D882 using a universal testing machine (Instron model 5567, USA) at 12.5 mm/min of crosshead

speed and 1 kN of load cell. Films were prepared in the rectangular shape of 10 mm wide and 100 mm long.

Impact strength of the films was recorded according to ASTM D3420 using an impact testing machine (Digital impact tester, Toyoseiki, Japan). Films were prepared in a square with dimension of 100 x 100 mm². The 1.5 J of pendulum energy was used for this measurement.

Tear strength in both MD and TD directions of films was performed according to ISO 6383 using a tear testing machine (Digital Elmendorf type tearing tester model SA, SA-W, Toyoseiki, Japan). The samples were prepared into the dimension of 63 x 75 mm². The 16 N of pendulum was used.

3.3.6 Permeability properties

Oxygen permeation (OP) of films was measured according to ASTM D3985 using a Mocon OX-TRAN model 2/21 (USA) with oxygen flow rate of 40 cm³/min at 23 °C and 0% relative humidity. The sample area was 100 cm².

Water vapor permeation (WVP) of films was collected according to ASTM E398 using a Mocon PERMATRAN-W model 398 (USA) with nitrogen flow rate of 800 cm³/min at 37.8 °C and 90% relative humidity. The sample area was 50 cm².

For all mechanical and gas permeation testing, the thickness of film was 40±1.08 µm.

3.3.7 Characterization of crosslink reaction of PLA/NRL/DCP films

The crosslink between PLA and NR was confirmed by using Fourier Transform Infrared Spectroscopy (FTIR; Thermo Scientific Nicolet 6700, USA) with a resolution of $\pm 4 \text{ cm}^{-1}$ and an average scan of 100 in the wavelength of 450–4000 cm^{-1} . For PLA/NRL/DCP films, the free PLA was extracted from the films with dichloromethane at ambient temperature for 4 times, then insoluble fraction was compressed into thin film. All samples were dried in an oven to eliminate residual solvent and moisture before characterization. The trace of PLA in dried insoluble fraction referred to PLA crosslinked with NR [1].

3.3.8 Gel content

The degree of crosslinking of NR was measured by extraction method. The free PLA in PLA/NRL/DCP films was extracted with dichloromethane at ambient temperature for 24 hours, 4 times, then insoluble NR fraction was extracted with toluene for 24 hours. The remaining insoluble fraction was dried at 80 °C for 30 min and subsequently weighed [19]. The percent of gel content of blends was calculated as follows

$$\% \text{ gel content} = \frac{W_g}{W_o} \times 100 \quad (3.5)$$

where W_g and W_o were sample weights after and before extraction of NR with toluene.

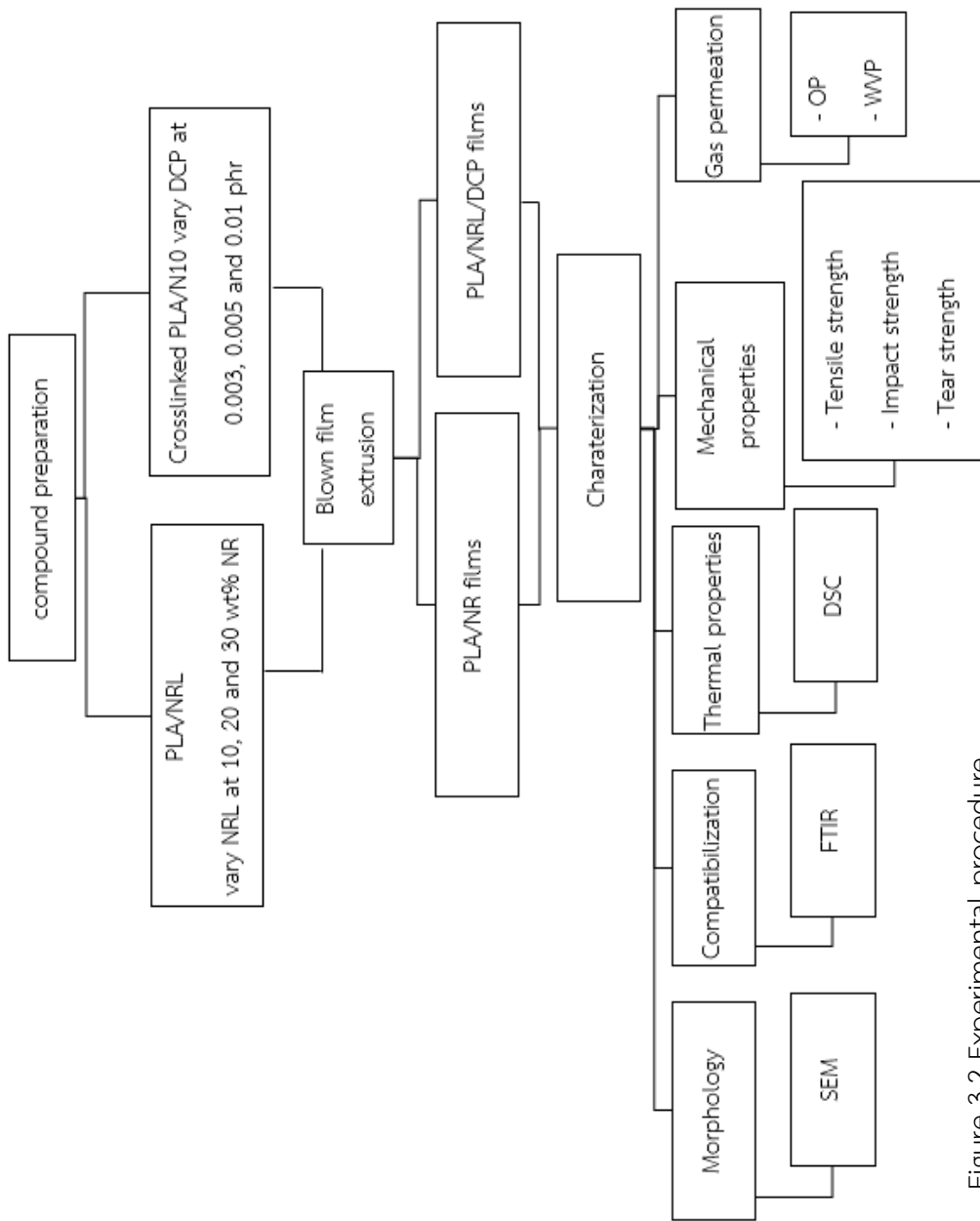


Figure 3.2 Experimental procedure

CHAPTER IV

RESULTS AND DISCUSSION

This study was designed to examine the relationship between the properties of PLA/NRL films and the amount of NRL content. The properties of PLA/NRL films after modification of interfacial adhesion by vulcanization using DCP were also evaluated.

PLA/N10 films provided higher transparency and smoother surface than PLA/ADS10 films. However, the films became highly opaque and exhibited rough surface with increasing NRL content to 30 wt% NR. Moreover, PLA/N10/DCP films were transparent but the surface was not as smooth as PLA/N10 films due to the self-crosslinked NR domains in the PLA matrix. The appearance of film for all composition is illustrated in Figure 4.1. The detail will be described in the latter section.

According to the rough surface and uneven film thickness, the average thickness of the film was calculated using equation 4.1. All average thickness of film was 40 ± 1.08 μm .

$$H = \frac{m}{\rho \times A} \times 10000 \quad (4.1)$$

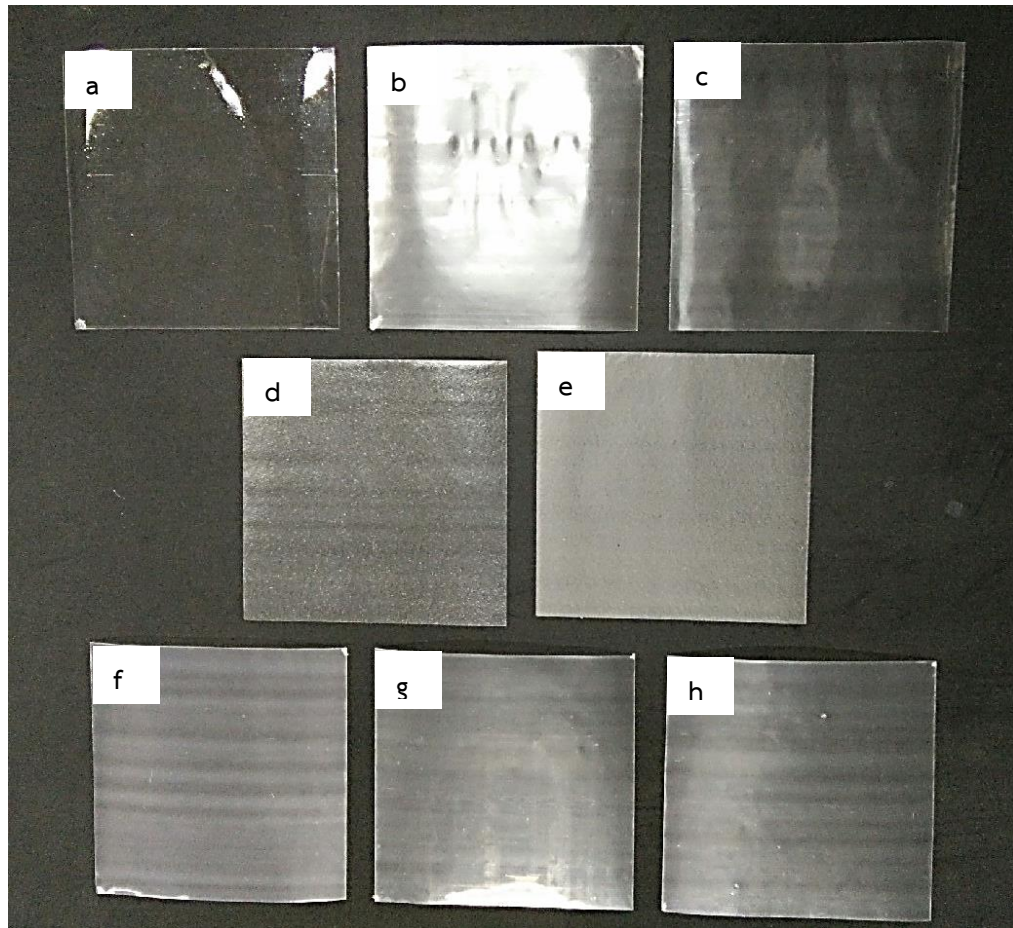
H = thickness of film (micrometer)

m = weight of film (g)

ρ = density of film (g/cm³)

A = area of film (cm²)





จุฬาลงกรณ์มหาวิทยาลัย
CHULALONGKORN UNIVERSITY

Figure 4.1 The appearance of films for all component a) neat PLA, b) PLA/ADS10
C) PLA/N10, d) PLA/N20, e) PLA/N30, f) PLA/N10/D0.003, g) PLA/N10/D0.005 and
h) PLA/N10/D0.01

4.1 Effect of rubber content on the properties of PLA/NRL films

4.1.1 Morphology

The morphology of PLA/NRL blown films in both machine direction (MD) and transverse direction (TD) was investigated by SEM as illustrated in Figure 4.2 and Figure 4.3, respectively. The low interfacial adhesion between PLA and NR led to the debonded NR domain during SEM preparation, then the cavitation would be observed on the PLA matrix [13]. Moreover, the size of NR domain and cavitation increased after addition of NR due to the coalescence of NR. It was clearly seen that the shape of NR domain in TD and MD were different. Namely, the shapes of NR domain from the cross-sectional fractured surface film in MD and TD were spherical and ellipsoidal, respectively. NR domains were pulled by nip roll in machine direction (MD) with stronger force than drawing by pneumatic force from an air flow inside bubble in TD.

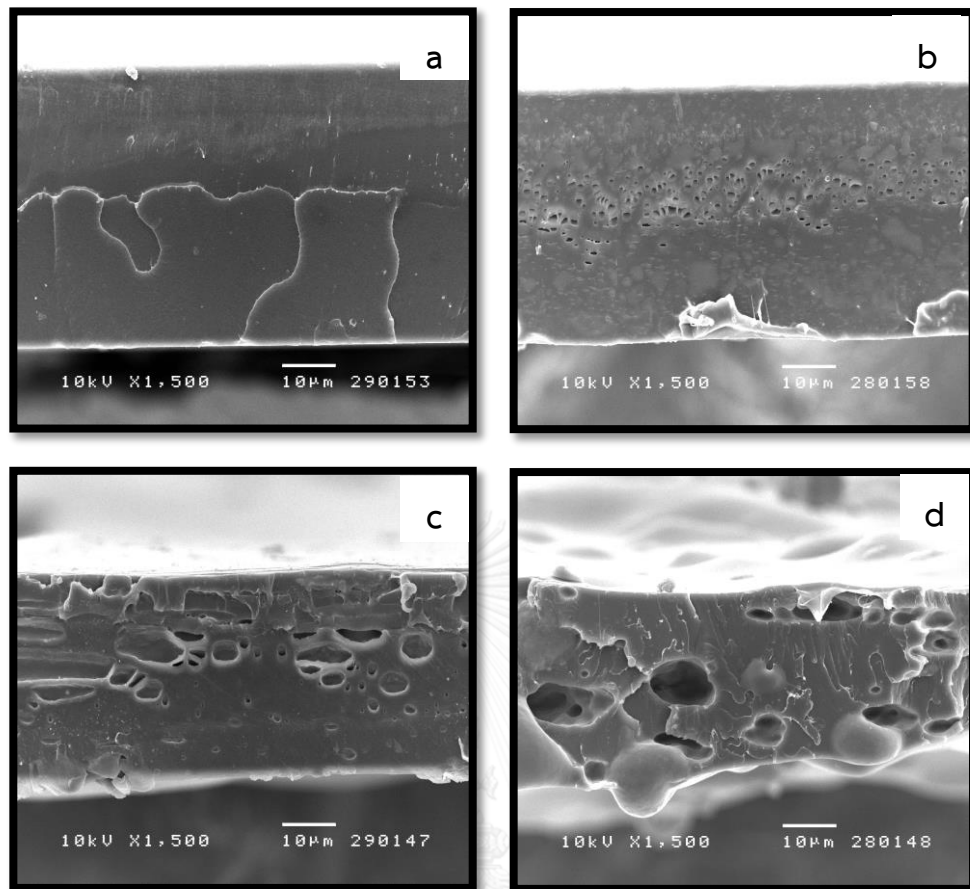


Figure 4.2 SEM micrograph of cross-sectional fractured surface in MD of a) neat PLA, b) PLA/N10, c) PLA/N20 and d) PLA/N30

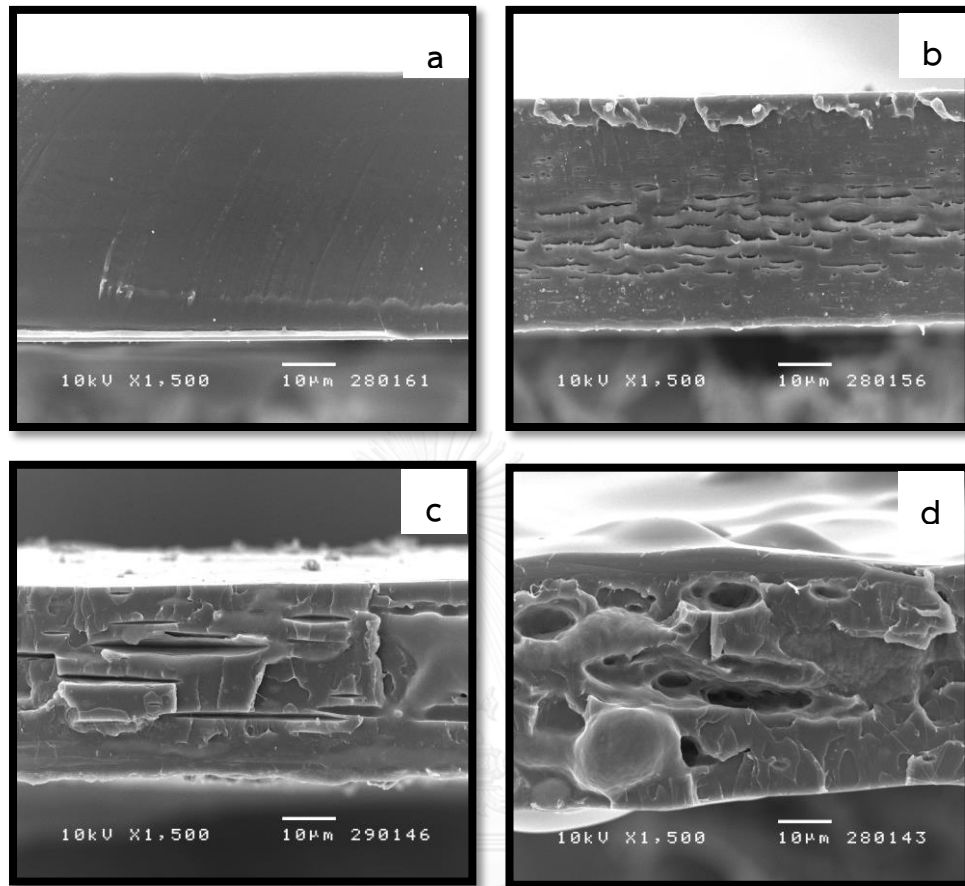


Figure 4.3 SEM micrograph of cross-sectional fractured surface in TD of a) neat PLA,

b) PLA/N10, c) PLA/N20 and d) PLA/N30

4.1.2 Thermal properties

The thermal properties and crystallization behavior of PLA and PLA/NRL films were recorded by dynamic DSC measurement in the second heating scan. The values of glass transition temperature (T_g), cold crystallization temperature (T_{cc}), melting temperature at low temperature (T_{m1}) and high temperature (T_{m2}), enthalpy of cold crystallization (ΔH_{cc}), enthalpy of melting (ΔH_m) and degree of crystallinity ($\%X_c$) were determined from the DSC profiles, which were tabulated in Table 4.1. It was clearly seen that the presence of NRL did not affect the T_g of PLA. T_g s of neat PLA and PLA/NRL films were approximately 55 °C, suggesting that PLA and NR were immiscible [12, 14]. T_{cc} of PLA/NRL films was higher than that of neat PLA implying that rubber restricted the mobility of PLA chain during cold crystallization upon heating [15]. Moreover, ΔH_{cc} of PLA/NRL film was lower than that of neat PLA, referring that an addition of NRL reduced the degree of crystallization during heating. The double melting peaks of neat PLA and PLA/NRL films were also observed by DSC thermograms.

The melting peak at high temperature (T_{m2}) refers to denser and more perfect crystalline structure than that at low temperature (T_{m1}) [20]. The loose crystals were melted and reorganized into the dense crystals, which subsequently remelted at high temperature [21]. The endothermic peak of PLA/N10 films showed the melting temperature between T_{m1} and T_{m2} . This might be due to the fact that the crystal structure of PLA is in between loose and dense crystals.

The addition of NRL increased degree of crystallinity ($\%X_c$) because NR may act as diluent agent on the crystallization of PLA by giving extra mobility of its chains to form crystal [22]. However, a large amount of NRL induced higher levels of free volume and tended to inhibit the crystal growth of PLA, resulting in low $\%X_c$ at PLA/N30 films [23]. Moreover, T_{m1} and T_{m2} showed no significant change with increasing NRL content. The DSC thermograms of PLA/NRL films from the first heating scan were illustrated in Appendix A.

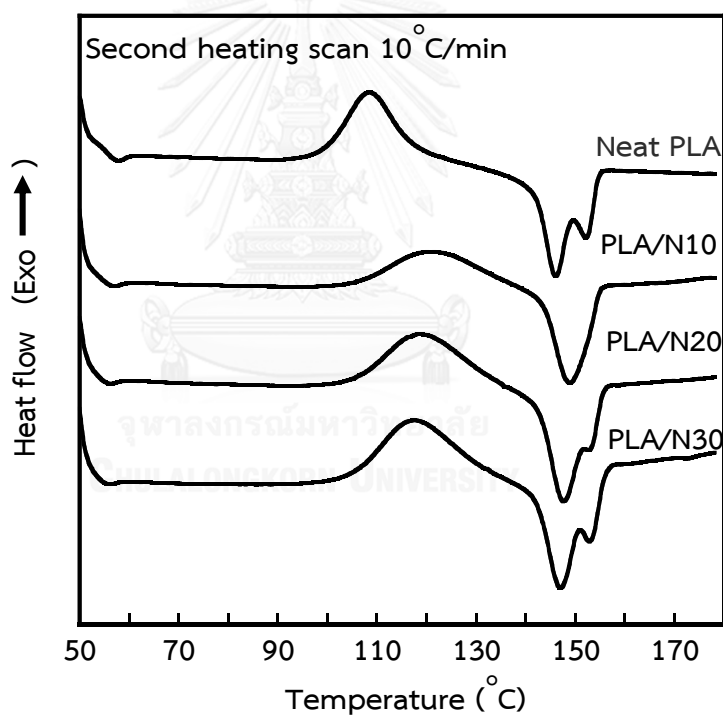


Figure 4.4 DSC thermograms in second heating scan of PLA/NRL blend

Table 4.1 Thermal properties of PLA/NRL blends in the second heating scan

Samples	T _g PLA (°C)	T _{cc} (°C)	T _{m1} (°C)	T _{m2} (°C)	ΔH _{cc} (J/g)	ΔH _m (J/g)	%X _c
Neat PLA	55.1	108.6	146.0	152.5	24.38	27.52	3.38
PLA/N10	55.0	122.5	150.3		14.49	21.88	8.83
PLA/N20	54.9	118.9	147.6	153.5	16.48	26.43	13.37
PLA/N30	54.3	117.2	147.1	153.5	23.86	26.29	3.37

4.1.3 Mechanical properties

The tensile properties in both transverse direction (TD) and machine direction (MD) of neat PLA and PLA/NRL films are shown in Figure 4.5- Figure 4.7 and the stress-strain curves are shown in Appendix B. The tensile strength and Young's modulus of neat PLA and PLA/NRL films at 10, 20 and 30 wt% NR are shown in Figure 4.5 and Figure 4.6, respectively. The tensile strength of neat PLA was higher than those of PLA/NRL films due to the brittleness of PLA and blending rubber with PLA also attributed the elasticity to the blended films [24]. The Young's modulus of films showed the same trend as tensile strength.

The elongation at break, tensile toughness and impact strength of PLA/NRL films increased when blending PLA with 10 wt% NR. Nonetheless, these values decreased with increasing NR up to 20 and 30 wt%. From the SEM micrographs, the domain size

of rubber become larger with increasing of NRL content dropping the ability of NR domain to absorb and dissipate the applied energy during measurements [8].

Tear strength of PLA/NRL films intensely decreased as a function of NRL content. Tear resistance depends on the domain size of dispersed phase and interfacial adhesion of binary blend. Namely, smaller domain sized rubber required higher energy to tear films [3]. Therefore, larger domain sized rubber of NR at higher NRL loading and poor interfacial adhesion between PLA and NR reduced the tear strength. Remarkably, the orientation of PLA chain and rubber domain parallel to machine direction (MD) was responsible for lower tear strength of films in MD. However, the tear testing in TD was required force to break films in perpendicular to the PLA chain orientation, resulting in higher tear strength in TD than that of MD [25]. The possible tear mechanisms were proposed in Figure 4.11.

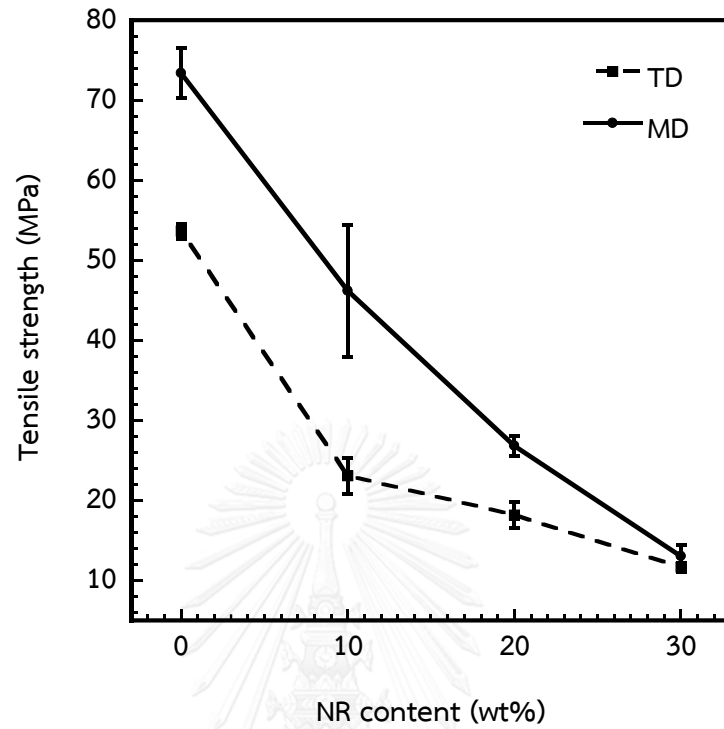


Figure 4.5 Tensile strength of neat PLA and PLA/NRL films

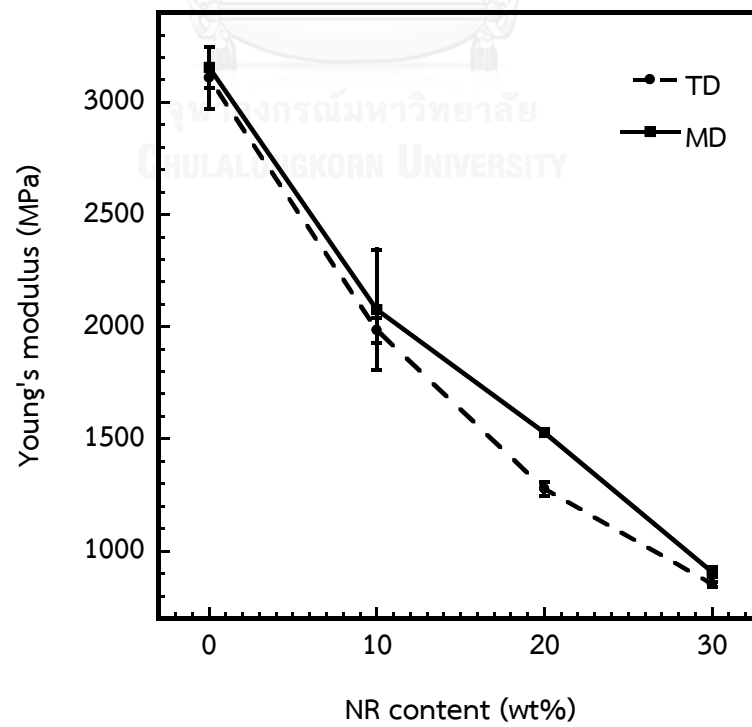


Figure 4.6 Young's modulus of neat PLA and PLA/NRL films

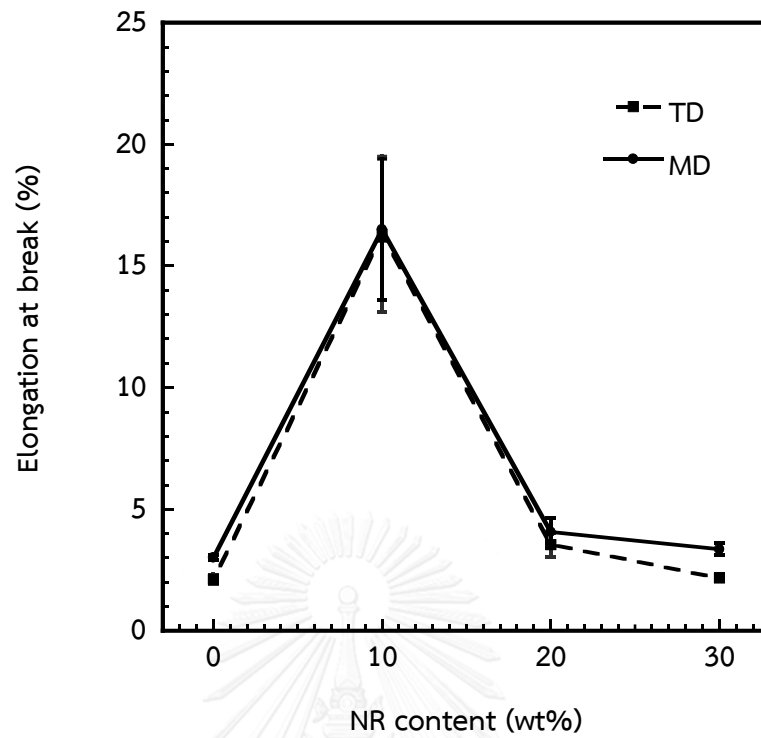


Figure 4.7 Elongation at break of neat PLA and PLA/NRL films

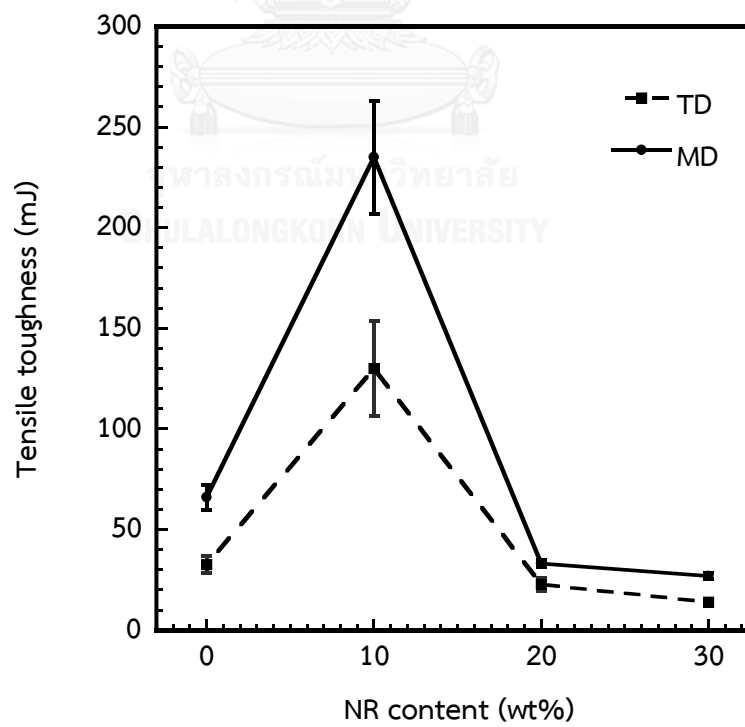


Figure 4.8 Tensile toughness of neat PLA and PLA/NRL films

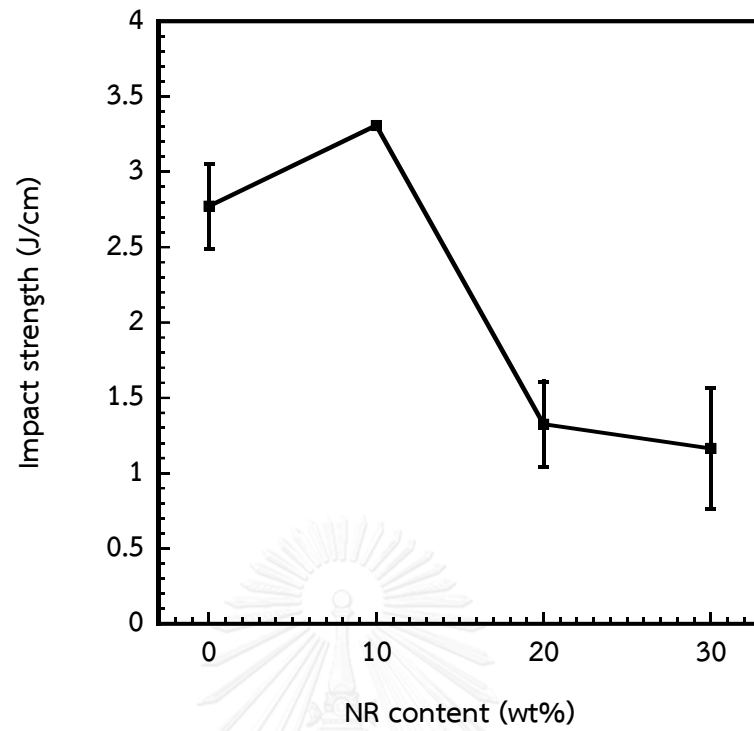


Figure 4.9 Impact strength of neat PLA and PLA/NRL films

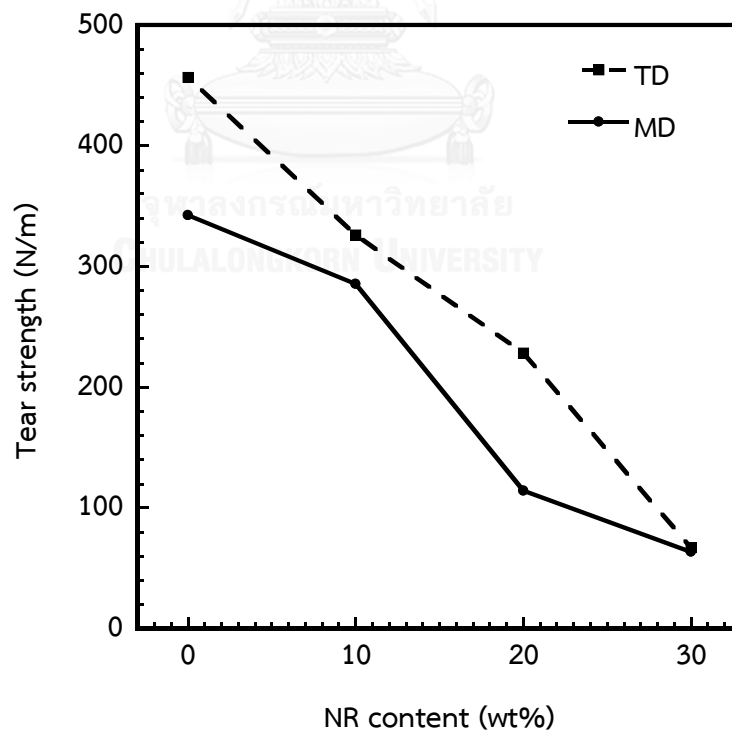


Figure 4.10 Tear strength of neat PLA and PLA/NRL films

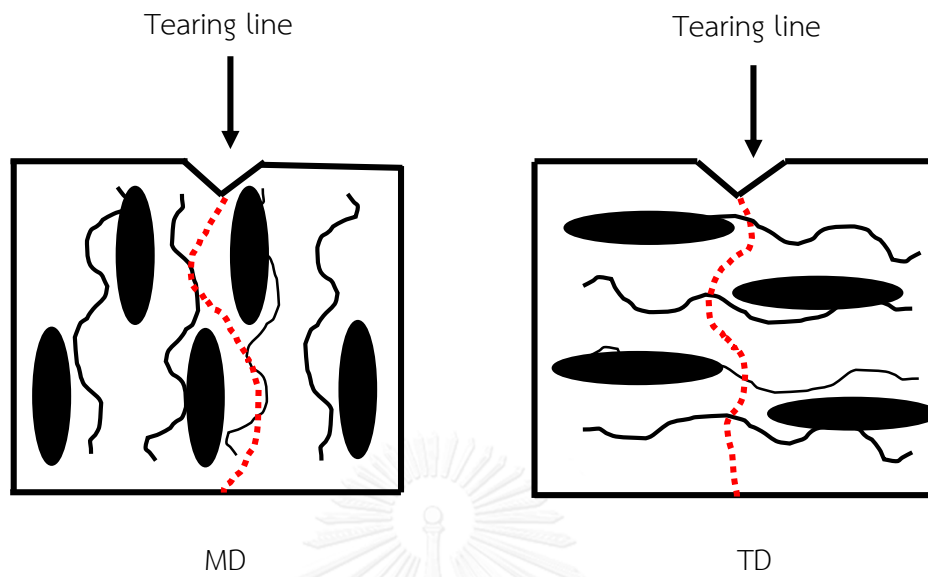


Figure 4.11 The possible tear mechanisms in PLA/NRL films [5]

4.1.4 Gas permeability

The water vapor permeation (WVP) and oxygen permeation (OP) of neat PLA films and PLA/NRL films with various contents of NRL are shown in Figure 4.12 and Figure 4.13, respectively. It was clearly seen that WVP and OP values linearly increased as a function of NRL because the poor interfacial adhesion between PLA and NR favored the microvoid formation at the interface formed upon film blowing process. The large domain size of rubber and the large amount of microvoids were formed at high NRL content. Moreover, the amorphous rubber had high free volume compared with PLA [5]. Hence, water vapor and oxygen easily passed through those microvoids and rubber free volume. It was remarkable that OP value drastically increased as a function of NRL because non polar oxygen molecules easily passed through the non-polar rubber phase [26].

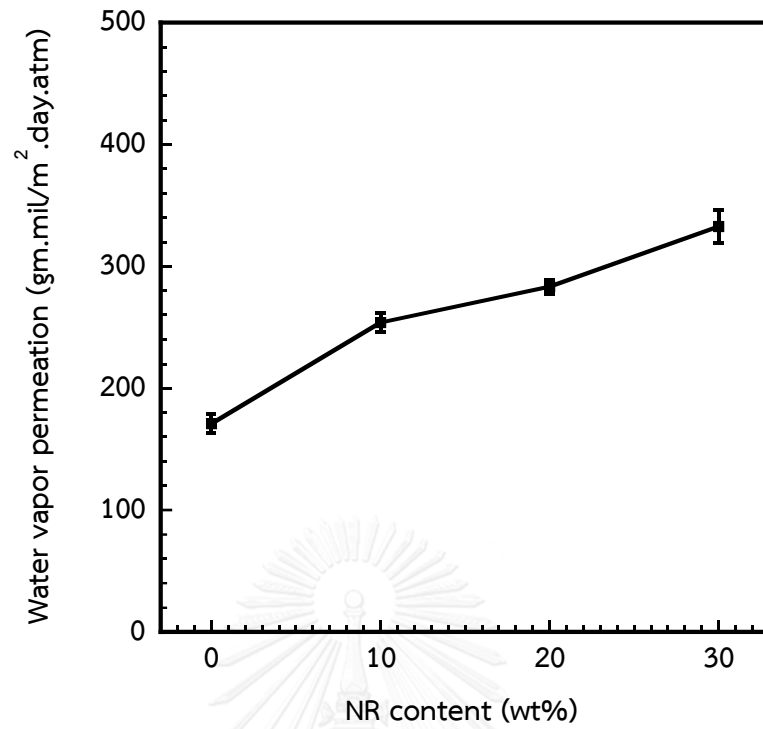


Figure 4.12 Water permeation of neat PLA and PLA/NRL films

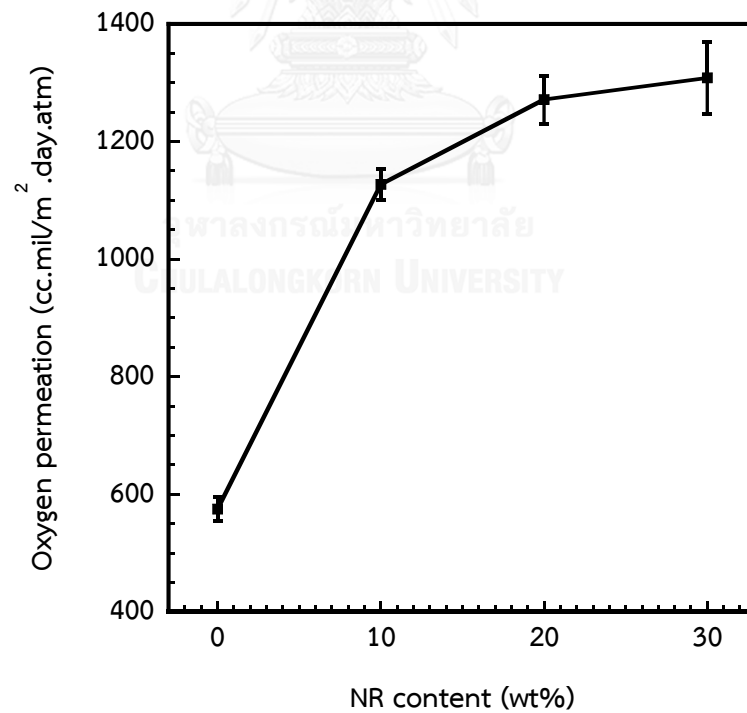


Figure 4.13 Oxygen permeation of neat PLA and PLA/NRL films

4.2 Effect of dynamic vulcanization by DCP on the properties of PLA/NRL/DCP films

It is worth mentioning that PLA/N10 was chosen for the dynamic vulcanization by DCP due to its highest mechanical properties such as elongation at break, tensile toughness and impact strength. The DCP content was varied at 0.003, 0.005 and 0.01 phr.

4.2.1 Morphology

The morphology of cross-sectional fractured surface in machine direction (MD) of PLA/N10/DCP films is illustrated in Figure 4.14. The data of domain size distribution of NR was tabulated in Table 4.2. The number average diameter (D_n) and volume average diameter (D_v) of NR domains of PLA/N10/DCP films were lower than those of PLA/N10 films. It was possible that the radicals from DCP coupled PLA chains and NR together. The formation of PLA-NR linkage acting as compatibilizer enhanced the interfacial adhesion. Therefore, NR domains are dispersed in PLA matrix rather than coalescence [9, 27]. However, when DCP content increased from 0.003 to 0.01, D_n and D_v of NR domains increased but polydispersity (PD) had no significant change. More cavities in PLA/N10/DCP films were observed at DCP content of 0.005 phr and 0.01 phr. It was possible that the crosslink reaction between NR and NR molecules was favorably occurred more than that of PLA and NR molecules. Consequently, some NR domains were easily removed during sample preparation for SEM. This phenomenon was also

confirmed with the morphology surface of PLA/N10/DCP in Figure 4.15. Therefore, the addition of DCP at 0.003 phr can improve the compatibility between PLA and NRL. In conversely, the effect was reversed as increasing DCP to 0.005 and 0.01 phr.

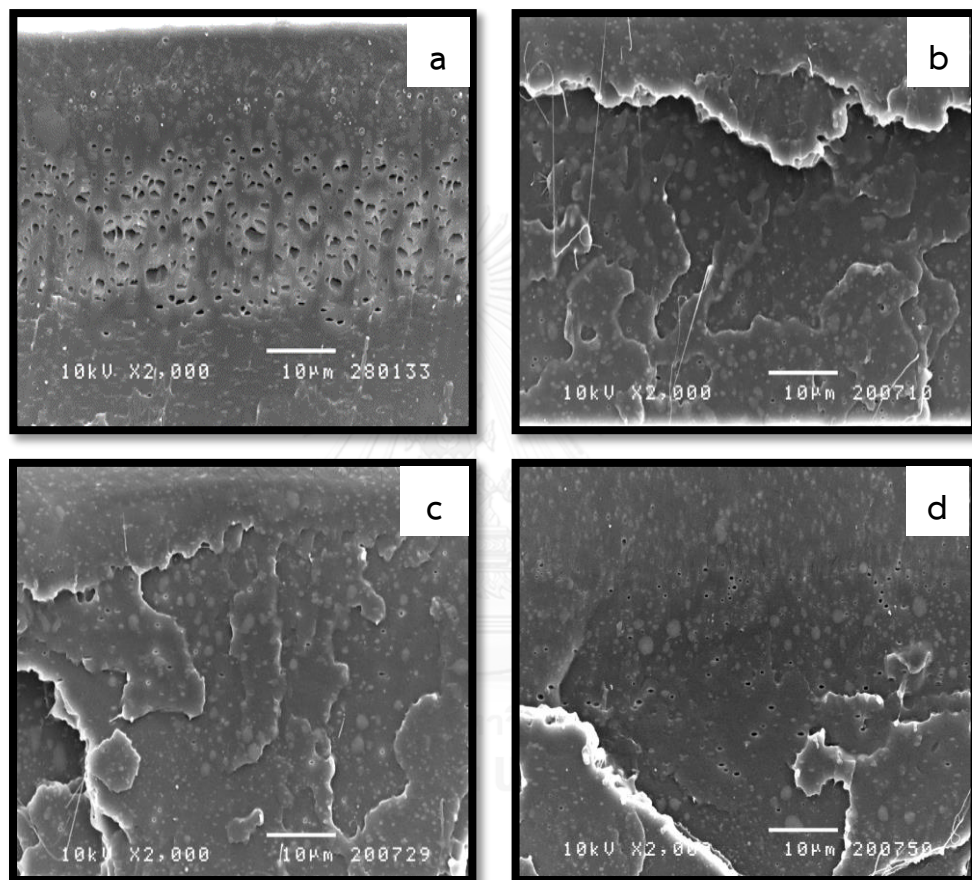


Figure 4.14 Morphology of cross-sectional fractured surfaces of PLA/N10/DCP films in MD at DCP content of a) 0 phr, b) 0.003 phr, c) 0.005 phr and d) 0.01 phr

Table 4.2 Number average diameter (D_n), volume average diameter (D_v) and polydispersity (PD) of PLA/N10/DCP films at different DCP contents

DCP (phr)	D_n (μm)	D_v (μm)	PD
0	1.56	5.23	3.80
0.003	0.46	0.92	2.01
0.005	0.60	1.22	2.05

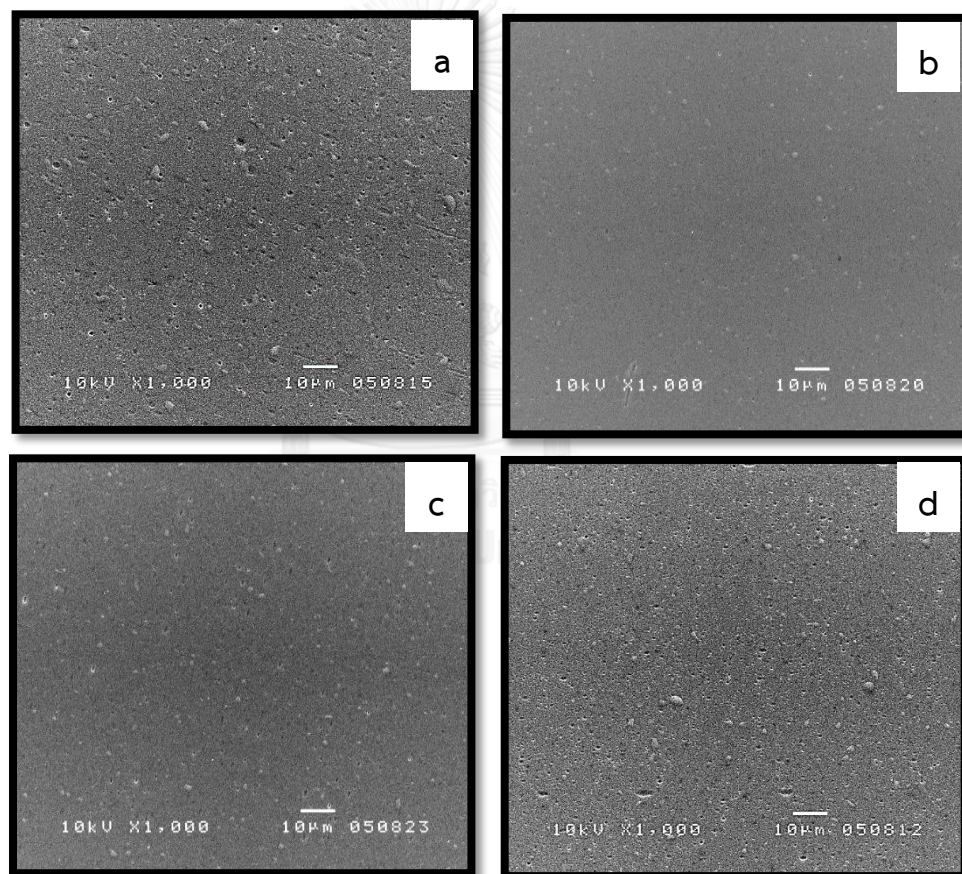


Figure 4.15 Morphology of surfaces of PLA/N10/DCP films at DCP content of a) 0 phr, b) 0.003 phr, c) 0.005 phr and d) 0.01 phr

4.2.2 Characterization of crosslink reaction of PLA/NRL/DCP films

The crosslink reaction between PLA and NR with different DCP contents was confirmed by FTIR technique. FTIR spectra of neat PLA, NRL and residual of dichloromethane-extracted PLA/N10 and PLA/N10/DCP films were recorded in a range of 450-4000 cm^{-1} as shown in Figure 4.16. FTIR spectrum of neat PLA showed the dominant absorption peak at 1753 cm^{-1} and 1180 cm^{-1} associated to the stretching vibration of carbonyl group (C=O) and C-O-C asymmetric, respectively [28]. Furthermore, the absorption band corresponding to =CH out-of-plane bending of natural rubber was observed at 835 cm^{-1} and the absorption band of CH_2 deformation at 1375 cm^{-1} [29]. The absorption peak at 1753 cm^{-1} was also observed in NRL due to the stretching vibration of carbonyl group of lipid in NRL [30]. The spectrum of residual of dichloromethane extracted PLA/N10 films was nearly identical to that of the pure NRL, indicating the complete removal of free PLA component during dichloromethane extraction. As a result, the crosslink reaction between PLA and NR did not occur in PLA/N10 films without DCP. However, the C-O-C stretching peak at 1180 cm^{-1} was clearly seen at the spectra of the residual of PLA/N10/DCP films, suggesting that crosslinked bonding between PLA and NR was formed during DCP induced crosslink reaction (dynamic vulcanization) at the melt blending process. The study of crosslink reaction between PLA and NR was also described by the ratio of absorption peak area at 1180 cm^{-1} to that at 1375 cm^{-1} ($A_{\text{PLA}}/A_{\text{NR}}$) as shown in Table 4.3. The $A_{\text{PLA}}/A_{\text{NR}}$ values tended to decrease with increasing DCP content because the ability of crosslink reaction

between PLA and NR was decreased, as a result of more favorable NR self-croslink reaction [31]. The FTIR results were complementary with the SEM micrographs. Namely, the addition of suitable amount of DCP in the PLA/N10 films can improve the compatibility between PLA and NR. On the contrary, those compatibilizations were decreased when too much DCP was added.

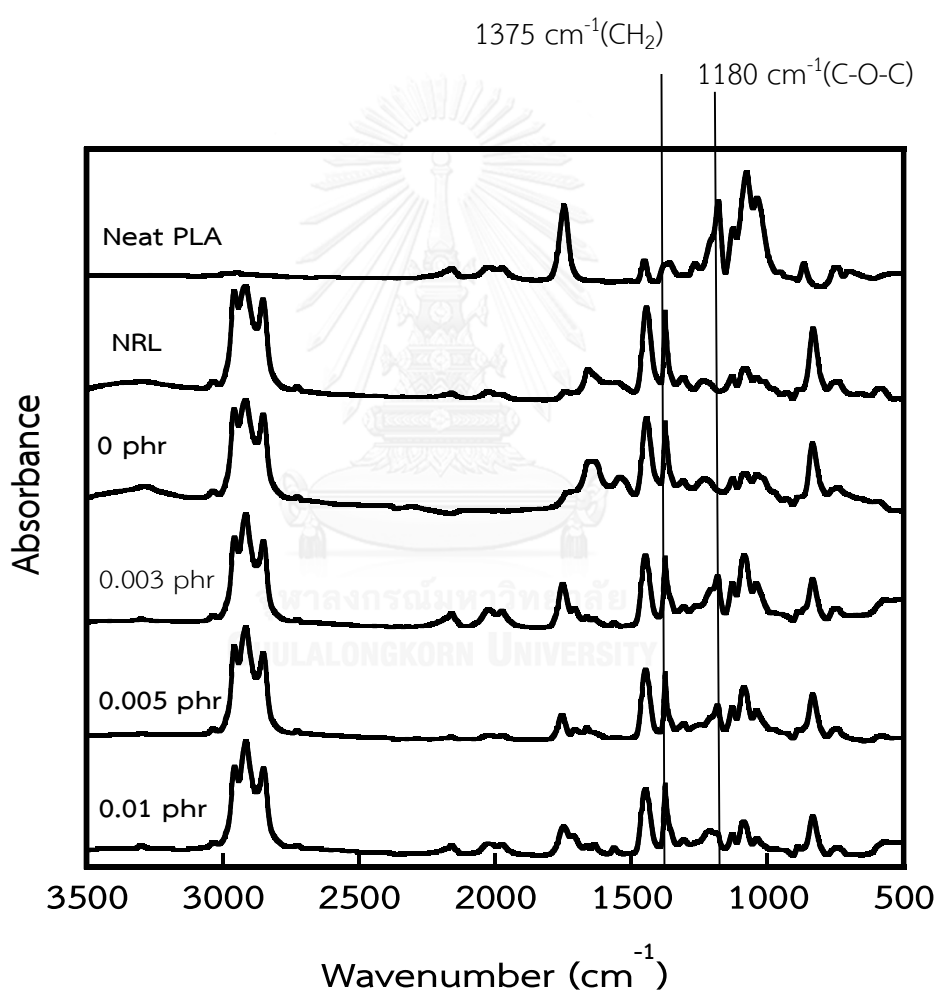


Figure 4.16 FTIR absorption spectra of neat PLA, NRL and residual of dichloromethane-extracted PLA/N10/DCP at DCP content of 0.003, 0.005 and 0.01 phr

Table 4.3 The ratio of absorption peak area ($A_{\text{PLA}}/A_{\text{NR}}$) of the residual of PLA/N10/DCP films at different DCP contents

DCP content (phr)	PLA		NR		$A_{\text{PLA}}/A_{\text{NR}}$
	Wave number (cm^{-1})	A_{PLA}	Wave number (cm^{-1})	A_{NR}	
0	0	0	1375.20	655.72	0
0.003	1180.76	496.44	1375.61	670.14	0.74
0.005	1180.34	448.59	1375.41	646.59	0.69
0.01	1180.50	231.99	1375.38	554.88	0.42

4.2.3 Gel content

The NR self-crosslink reaction was confirmed by a measurement of the gel content as illustrated in Table 4.4. Gel content tended to increase with increasing DCP content because DCP favored the NR self-crosslink reaction. Therefore, the ability of crosslink reaction between PLA and NR was decreased in an agreement with the FTIR results.

Table 4.4 Gel content of PLA/N10/DCP films at different DCP contents

PLA/N10/DCP at DCP content of (phr)	Gel content (%)
0.003	36.03
0.005	51.35
0.01	58.85

4.2.4 Thermal properties

The DSC thermograms of PLA/N10/DCP films from the second heating scan were illustrated in Figure 4.17. The thermal properties were tabulated in Table 4.5. T_g of PLA/N10/DCP films at DCP content of 0.003 phr decreased from 55.0 °C to 51.7 °C in which it was shifted to the T_g of natural rubber which is about -65 °C [32]. It would be due to some interaction between PLA and NR. However, when further increase DCP content, the T_g of PLA/N10/DCP films shifted to higher value (close to neat PLA), indicating the decrease in efficiency of crosslink reaction. T_{cc} and ΔH_{cc} of PLA/N10/DCP films had no significant change from those of PLA/N10 films. The value of $\%X_c$ of PLA/N10/DCP films was lower than those of PLA/N10 films because the crosslink between PLA and NR suppressed molecular motion for crystallization of PLA chain [33]. Moreover, T_m , ΔH_{cc} , ΔH_m and $\%X_c$ showed no significant change with increasing DCP content. The DSC thermograms of PLA/N10/DCP films from the first heating scan were illustrated in Appendix A.

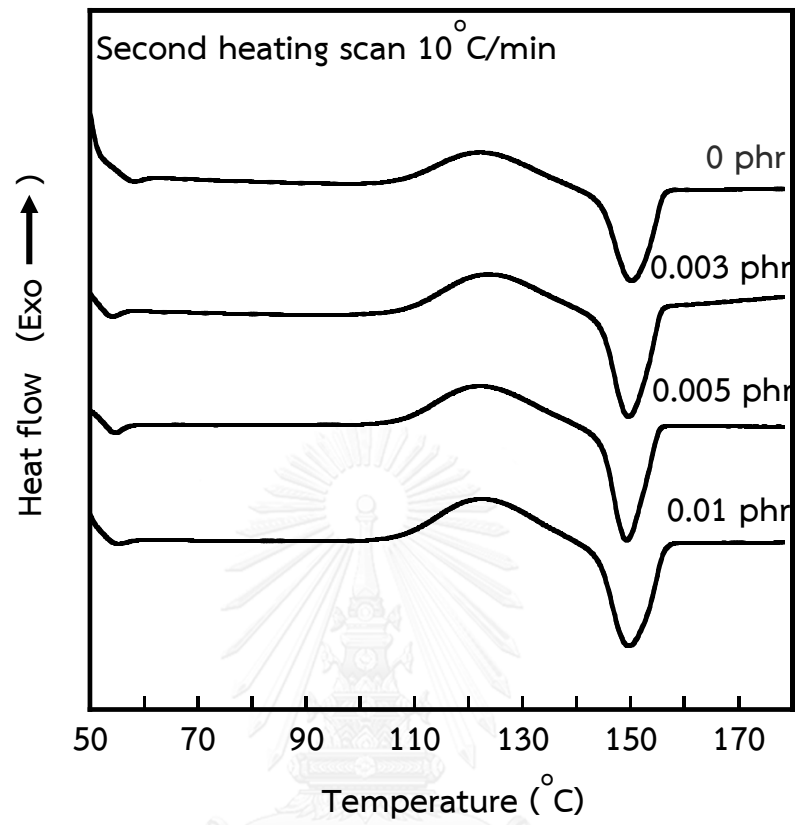


Figure 4.17 DSC thermograms in the second heating scan of PLA/N10/DCP blends

Table 4. 5 Thermal properties of PLA/N10/DCP blends in the second heating scan

DCP content (phr)	$T_{g\text{ PLA}}$ (°C)	T_{cc} (°C)	T_m (°C)	ΔH_{cc} (J/g)	ΔH_m (J/g)	% X_c
0	55.0	122.5	150.3	14.49	21.88	8.83
0.003	51.7	124.1	149.6	15.35	19.33	4.76
0.005	53.0	123.2	149.3	15.84	19.93	4.89
0.01	53.8	123.2	149.6	15.79	19.95	4.97

The DSC results indicated that the addition of DCP in the PLA/N10 films can improve the interaction between PLA and NR. The morphology results showed that the rubber domain size of PLA/N10/DCP films were smaller than that of PLA/N10 films. Also, the absorbance peak of carbonyl group were appeared in extracted dichloromethane films suggesting the crosslink reaction between PLA and NR. Moreover the T_g value of PLA/N10/DCP films slightly shift to lower value.

In contrary, the addition of DCP at 0.005 and 0.01 phr showed reverse effect to rubber domain size, T_g value and the ratio of peak area ($A_{\text{PLA}}/A_{\text{NR}}$) which refer to the compatibility between PLA and NR.

4.2.5 Mechanical properties

The tensile properties in both transverse direction (TD) and machine direction (MD) of PLA/N10/DCP films are shown in Figure 4.18-Figure 4.21. PLA/N10/DCP film with 0.003 phr of DCP content showed the highest mechanical properties. The tensile strength and Young's modulus of PLA/N10 films and PLA/N10/DCP films were shown in Figure 4.18 and Figure 4.19, respectively. The tensile strength and Young's modulus of PLA/N10/DCP films were higher than those of PLA/N10 films due to the improved interfacial adhesion between PLA and NR. However, the tensile strength and Young's modulus decreased with increasing DCP content due to less compatibility between PLA and NR as a result of self-crosslink of NR domains. Also, the larger domain sized rubber led to reduced force used for drawing the sample before plastic deformation in tensile test. Nevertheless, the tensile strength and Young's modulus of PLA/N10/DCP films were still higher than those of PLA/N10 films. The blends with DCP at 0.003 phr had high efficiency to induce the compatibility between PLA and NR and the smaller domain sized rubber was more effective to absorb and dissipate energy, resulting in increased mechanical properties.

The elongation at break and tensile toughness of PLA/N10 films and PLA/N10/DCP films are depicted in Figure 4.20 and Figure 4.21, respectively. The elongation at break and tensile toughness of PLA/N10/DCP films showed the same trend as their tensile strength and Young's modulus. Nonetheless, increasing DCP higher than 0.003 phr resulted in lower elongation at break and Young's modulus than

PLA/N10 films due to poor interfacial adhesion because the crosslink reaction between NR and NR was probably occurred at higher DCP content.

The impact strength of PLA/N10/DCP films was higher than that of PLA/N10 films. However, the efficiency of absorption and dissipation energy was dropped due to the large domain sized rubber and poor interfacial adhesion as increasing DCP content as shown in Figure 4.22.

The tear strength was shown in Figure 4.23. The tear strength value also tend to increase with the addition of DCP content in PLA/N10 films because the sample required higher force to tear the film as a result of the interfacial adhesion which was improved by crosslinked reaction between PLA and NR. Thus, the PLA/N10 film with DCP at 0.005 and 0.01 phr would require the lower force to tear the sample than those of PLA/N10/DCP at DCP content of 0.003 phr.

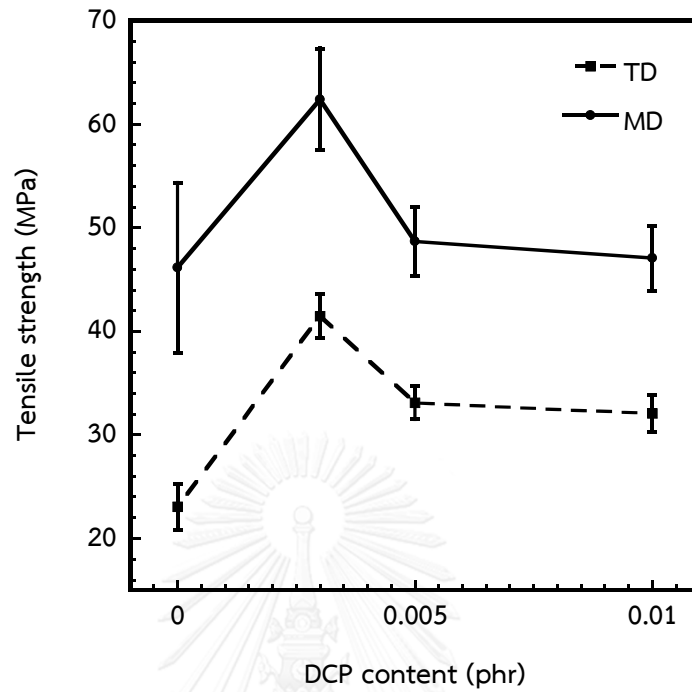


Figure 4.18 Tensile strength of PLA/N10 with DCP content of 0.003, 0.005 and 0.01 phr

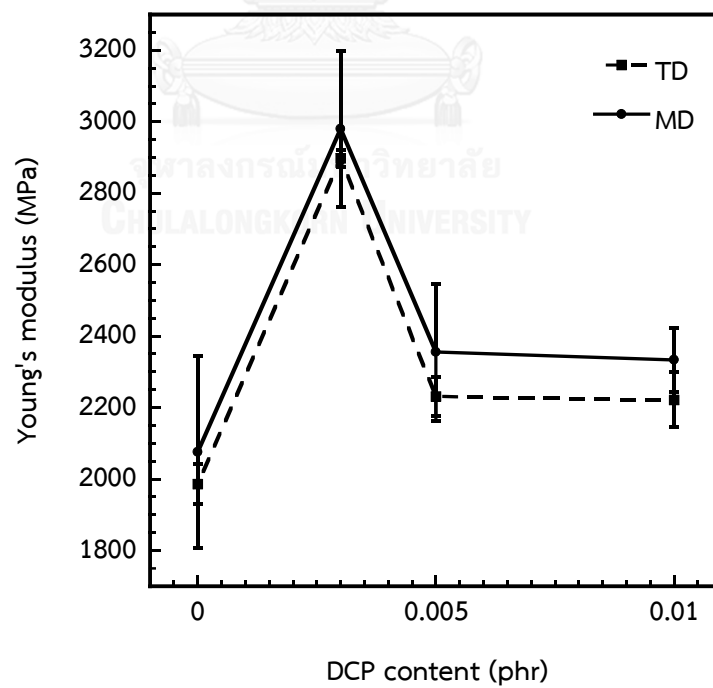


Figure 4.19 Young's modulus of PLA/N10 with DCP content of 0.003, 0.005 and 0.01 phr

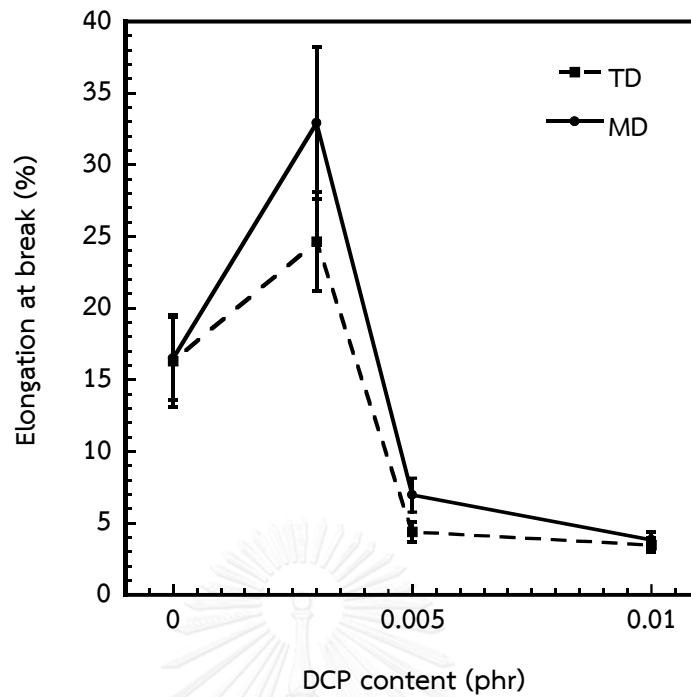


Figure 4.20 Elongation at break of PLA/N10 with DCP content of 0.003, 0.005 and 0.01 phr

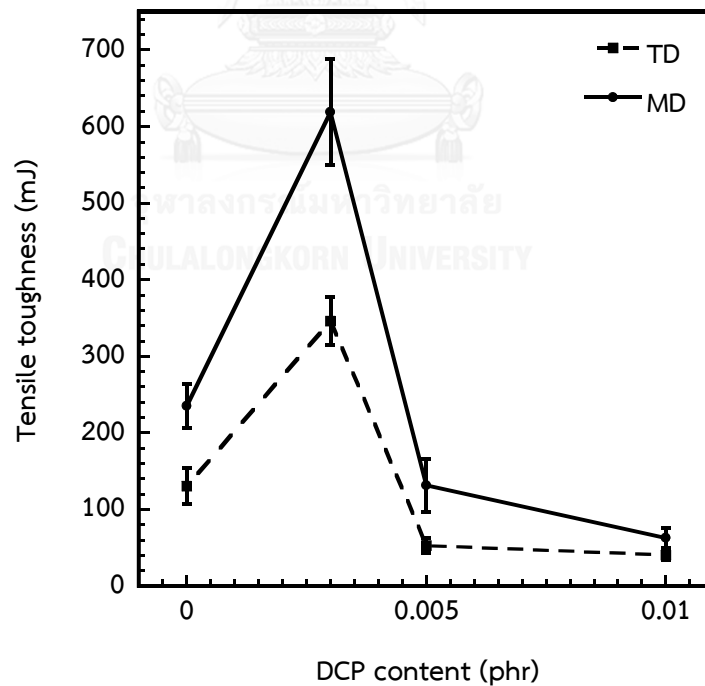


Figure 4.21 Tensile toughness of PLA/N10 with DCP content of 0.003, 0.005 and 0.01 phr

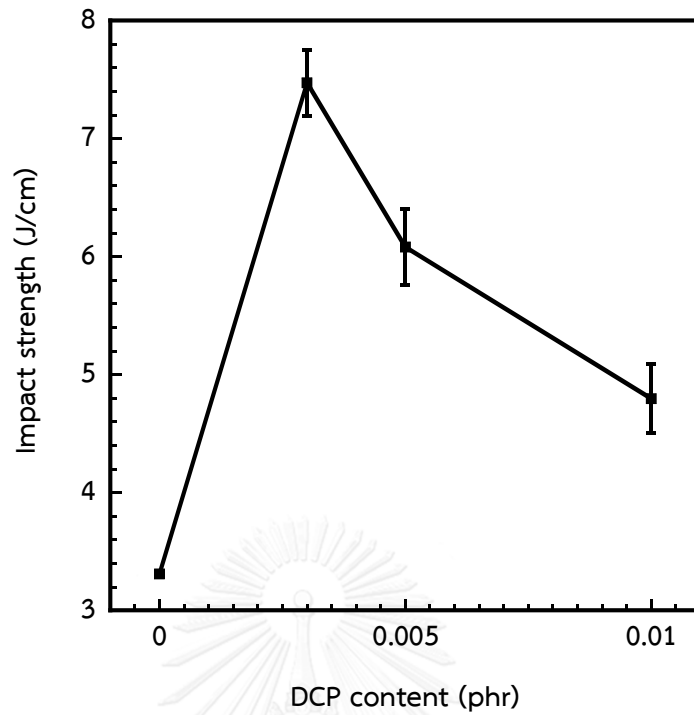


Figure 4.22 Impact strength of PLA/N10 with DCP content of 0.003, 0.005 and 0.01 phr

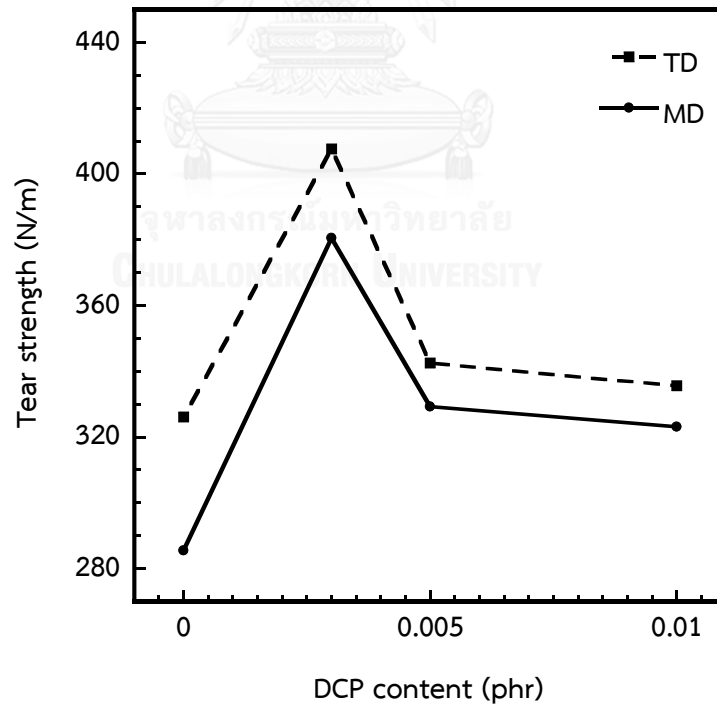
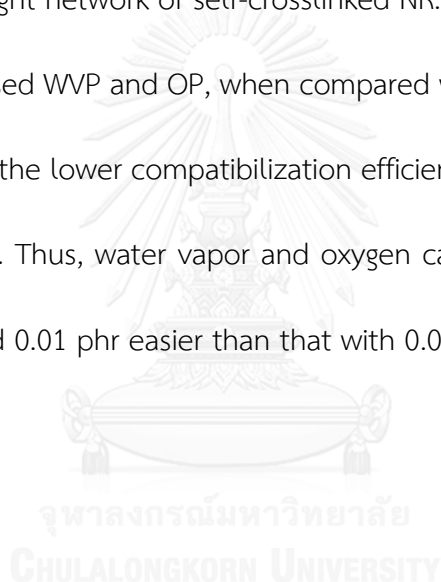


Figure 4.23 Tear strength of PLA/N10 with DCP content of 0.003, 0.005 and 0.01 phr

4.2.6 Gas permeability

The values of WVP and OP of PLA/N10 films and PLA/N10/DCP films are shown in Figure 4.24 and Figure 4.2, respectively. The WVP and OP values of PLA/N10/DCP films were lower than those of PLA/N10 films, owing to the improvement of compatibility between PLA and NR. The good interfacial adhesion was represented by smaller amount of microvoids as well as oxygen and water vapor molecules hardly penetrated through tight network of self-crosslinked NR. Nonetheless, further addition of DCP slightly increased WVP and OP, when compared with PLA/N10 film with DCP at 0.003 phr because of the lower compatibilization efficiency of the interfacial adhesion between PLA and NR. Thus, water vapor and oxygen can pass through PLA/N10 film with DCP of 0.005 and 0.01 phr easier than that with 0.003 phr of DCP.



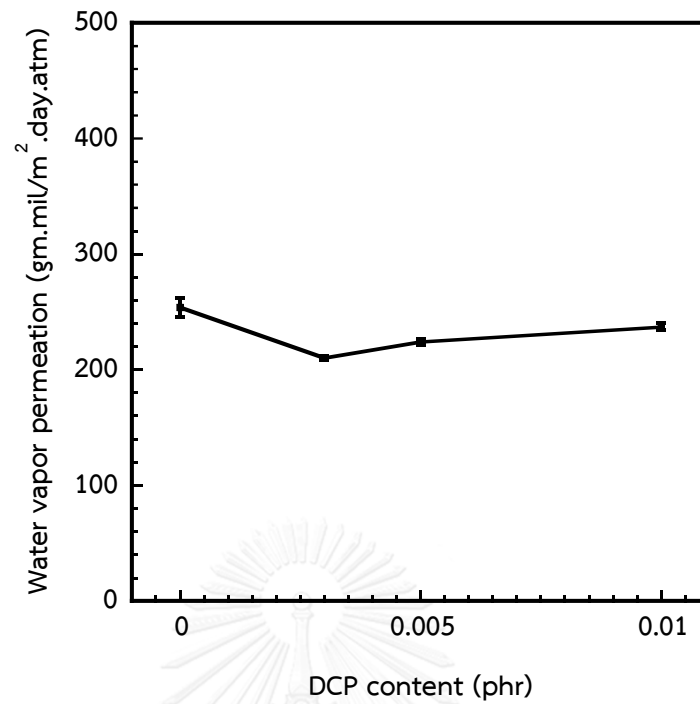


Figure 4.24 Water vapor permeation of PLA/N10 with DCP content of 0.003, 0.005 and 0.01 phr

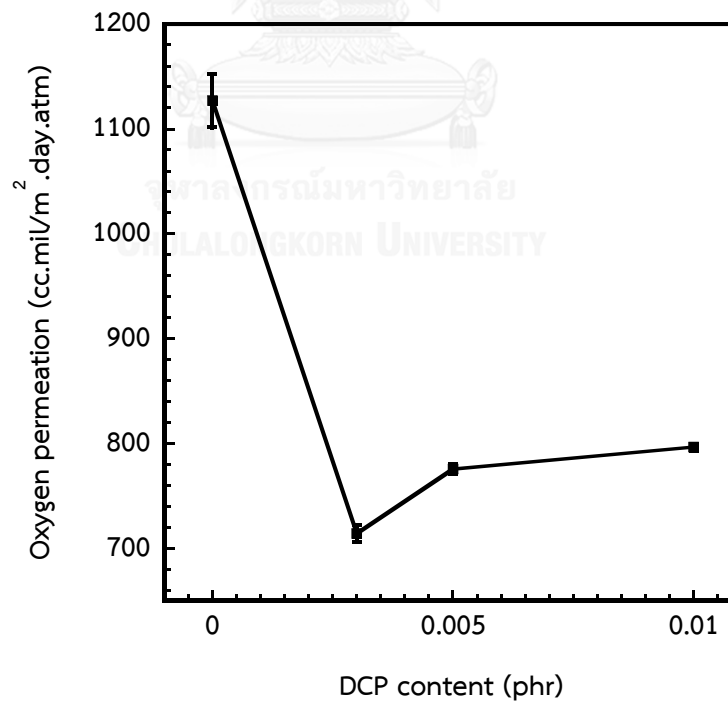


Figure 4.25 Oxygen permeation of PLA/N10 with DCP content of 0.003, 0.005 and 0.01 p

CHAPTER V

CONCLUSIONS AND RECOMMENDATIONS

5.1 Conclusions

This research aimed to improve the mechanical properties of PLA blown film by incorporation with natural rubber latex (NRL) and to improve the interfacial adhesion between PLA and NR by using dicumyl peroxide (DCP) as curing agent.

In this study, PLA could be melt-mixed with NRL up to 30 wt% dried rubber content (NR). The higher than 30 wt% NR blending in PLA cannot be achieved due to low melt strength of bubble during blown film process. The morphology result showed that domain sized of rubber increased with increasing NRL content due to the coalescence of NR domains. In addition, the thermal properties strongly confirmed the immiscibility of PLA and NR as T_g value did not change as increasing NRL content. Dispersed NR domain could hinder the crystallization of PLA chain. Thus, the degree of crystallinity of PLA/NRL blend was lower than that of neat PLA. The elongation at break, tensile toughness and impact strength of PLA/NRL films were improved by blending PLA with NRL at 10 wt% NR. Nevertheless, the mechanical properties tended to decrease as NRL content further increases. The WVP and OP values linearly

increased as a function of NRL due to the increase microvoid formation from poor interfacial adhesion between PLA and NR.

In order to improve the mechanical properties of PLA/NRL films, the interfacial adhesion between PLA and NR was improved by adding DCP as curing agent. Herein, the PLA/N10 films was selected in this part because PLA/N10 films had the highest mechanical properties. From morphology result, it indicated that the addition of DCP induced smaller domain sized rubber and less cavity, comparing with the system without any addition of DCP. In contrary, the inverse effect of domain sized rubber and the number of cavitation were occurred with increasing DCP content. The appearance of C-O-C absorbance peak of PLA in the residual sample from the PLA extraction suggesting the crosslink reaction between PLA and NR. On the other hand, further increasing DCP content led to a reduction of area ratio of PLA to NR ($A_{\text{PLA}}/A_{\text{NR}}$). The thermal properties of films confirmed the crosslink reaction between PLA to NR as T_g of PLA slightly shifted closer to T_g of NRL. On the contrary, the T_g of PLA/N10/DCP films shifted to higher value with further increasing DCP content, indicating that the efficiency of crosslink reaction would drop with increasing DCP content to 0.005 and 0.01 phr. PLA/N10/DCP films had the highest mechanical properties at DCP content of 0.003 phr. Moreover, the mechanical properties of PLA/N10/DCP films were higher than those of PLA/N10 films without any addition of DCP, except the elongation at break and toughness of PLA/N10/DCP films at 0.005 and 0.01 phr of DCP which were lower than those of PLA/N10 films. The WVP and OP of PLA/N10/DCP films were lower than those

of PLA/N10 films due improved interfacial adhesion. However, WVP and OP tended to increase with further increasing DCP due to low efficiency of compatibilization as described previously. Accordingly, the mechanical properties of PLA/N10 film can improved with crosslink reaction between PLA and NR induced by DCP at 0.003 phr.

Herein, at low NRL content the films with outstanding oxygen and water vapor permeation are suitable to be used as green permeable packaging to preserve the agricultural products with high respiration rate such as straw mushroom. On the other hand, at high NRL content the films with low oxygen and high water vapor permeation can be used as barrier film for green vegetable such as Parsley and Celery.

5.2 Recommendations

- Other peroxide should be studied because the initiation rate of peroxide could affect the vulcanization rate.

REFERENCES

- [1] Yuan, D., Chen, K., Xu, C., Chen, Z., and Chen, Y. Crosslinked bicontinuous biobased PLA/NR blends via dynamic vulcanization using different curing systems. Carbohydrate Polymer 113 (2014): 438-445.
- [2] Weng, Y.-X., Jin, Y.-J., Meng, Q.-Y., Wang, L., Zhang, M., and Wang, Y.-Z. Biodegradation behavior of poly(butylene adipate-co-terephthalate) (PBAT), poly(lactic acid) (PLA), and their blend under soil conditions. Polymer Testing 32(5) (2013): 918-926.
- [3] Numpiboonmarn, P. Effects of mastication time and type of natural rubber on properties of poly(lactic acid)/natural rubber blown films. Master degree, Chemical Engineering Chulalongkorn University, 2013.
- [4] Ketwattha, U. The development of toughness and gas permeability of poly(lactic acid)/maleic anhydride-g-natural rubber blown film. Master degree, Chemical Engineering Chulalongkorn University, 2011.
- [5] Jaitrong, N. Properties of poly(lactic acid)/natural rubber/thermoplastic starch blown films. Master degree, Chemical Engineering Chulalongkorn University, 2013.
- [6] Tantipiriyakij, P. and Suwanpimolkul, P. Usage of natural rubber latex in the compounding process of poly(lactic acid) blown film. Bachelor degree, Chemical Engineering Chulalongkorn University, 2011.

- [7] Ishida, S., Nagasaki, R., Chino, K., Dong, T., and Inoue, Y. Toughening of poly(L-lactide) by melt blending with rubbers. Journal of Applied Polymer Science 113(1) (2009): 558-566.
- [8] Jaratrotkamjorn, R., Khaokong, C., and Tanrattanakul, V. Toughness enhancement of poly(lactic acid) by melt blending with natural rubber. Journal of Applied Polymer Science (2012): 5027-5036.
- [9] Ma, P., Hristova-Bogaerds, D.G., Lemstra, P.J., Zhang, Y., and Wang, S. Toughening of PHBV/PBS and PHB/PBS blends via in situ compatibilization using dicumyl peroxide as a free-radical grafting initiator. Macromolecular Materials and Engineering 297(5) (2012): 402-410.
- [10] Mangmeemak, J. The development of poly(lactic acid) packaging films with natural rubber. Master degree, Chemical Engineering Chulalongkorn University, 2011.
- [11] Pongtanayut, K., Thongpin, C., and Santawitee, O. The effect of rubber on morphology, thermal properties and mechanical properties of PLA/NR and PLA/ENR blends. Energy Procedia 34 (2013): 888-897.
- [12] Bitinis, N., Verdejo, R., Cassagnau, P., and Lopez-Manchado, M.A. Structure and properties of polylactide/natural rubber blends. Materials Chemistry and Physics 129(3) (2011): 823-831.

- [13] Xu, C., Yuan, D., Fu, L., and Chen, Y. Physical blend of PLA/NR with co-continuous phase structure: Preparation, rheology property, mechanical properties and morphology. Polymer Testing 37 (2014): 94-101.
- [14] Liu, G.C., He, Y.S., Zeng, J.B., Li, Q.T., and Wang, Y.Z. Fully biobased and supertough polylactide-based thermoplastic vulcanizates fabricated by peroxide-induced dynamic vulcanization and interfacial compatibilization. Biomacromolecules 15(11) (2014): 4260-4271.
- [15] Yuan, D., Xu, C., Chen, Z., and Chen, Y. Crosslinked bicontinuous biobased polylactide/natural rubber materials: Super toughness, “net-like”-structure of NR phase and excellent interfacial adhesion. Polymer Testing 38 (2014): 73-80.
- [16] Huang, Y., Zhang, C., Pan, Y., Wang, W., Jiang, L., and Dan, Y. Study on the effect of dicumyl peroxide on structure and properties of poly(lactic acid)/natural rubber blend. Journal of Polymers and the Environment 21(2) (2012): 375-387.
- [17] Lin, Z., Xinhua, X., Ning, Y., Na, S., and Jing, S. Influence of composition and phase morphology on rheological properties of polypropylene/ poly(ethylene-co-octene) blends. Polymer composites 31 (2010): 105-113.
- [18] Suksut, B. and Deeprasertkul, C. Effect of nucleating agents on physical properties of poly(lactic acid) and its blend with natural rubber. Journal of Polymers and the Environment 19(1) (2010): 288-296.
- [19] Halimatuddahlia, Ismail, H., and Akil, H.M. The Effect of Dicumyl Peroxide Vulcanization on the Properties & Morphology of Polypropylene/Ethylene-

- Propylene Diene Terpolymer/Natural Rubber Blends. International Journal of Polymeric Materials 54(12) (2005): 1169-1183.
- [20] Cocca, M., Lorenzo, M.L.D., Malinconico, M., and Frezza, V. Influence of crystal polymorphism on mechanical and barrier properties of poly(l-lactic acid). European Polymer Journal 47(5) (2011): 1073-1080.
- [21] Sarasua, J.-R., E., P.h., WisniewskiMuriel, Le, B.A., and Nicolas, S. Crystallization and melting behavior of polylactides. Macromolecules 31 (1998): 3895-3905.
- [22] Chen, J.-H., Tsai, F.-C., Nien, Y.-H., and Yeh, P.-H. Isothermal crystallization of isotactic polypropylene blended with low molecular weight atactic polypropylene. Part I. Thermal properties and morphology development. Polymer 46(15) (2005): 5680-5688.
- [23] Zaman, H.U., et al. Poly(lactic acid) blends with desired end-use properties by addition of thermoplastic polyester elastomer and MDI. Polymer Bulletin 67(1) (2011): 187-198.
- [24] Kaavessinaa, M. and I. Alic, S.M.A.-Z. The influences of elastomer toward crystallization of poly(lactic acid). Procedia Chemistry 4 (2012): 164-171.
- [25] Wongchaichana, T. Effect of film blowing and drawing conditions on properties of poly(lactic acid)/natural rubber films. Master degree, Chemical Engineering Chulalongkorn University, 2013.

- [26] Bijarimi, M., Ahmad, S., and Rasid, R. Melt blends of poly(lactic acid)/natural rubber and liquid epoxidised natural rubber. Journal of Rubber Research 17 (2015): 57-68.
- [27] Wei, Q., Chionna, D., Galoppini, E., and Pracella, M. Functionalization of LDPE by melt grafting with glycidyl methacrylate and reactive blending with polyamide-6. Macromolecular Chemistry and Physics 204 (2003): 1123-1133.
- [28] Chieng, B.W., Ibrahim, N.A., Yunus, W.M.Z.W., and Hussein, M.Z. Poly(lactic acid)/poly(ethylene glycol) polymer nanocomposites: effects of graphene nanoplatelets. Polymer 6 (2014): 93-104.
- [29] Aieloa, P.B., et al. Evaluation of sodium diclofenac release using natural rubber latex as carrier. Materials Research 17 (2014): 146-152.
- [30] Rolere, S., Liengprayoon, S., Vaysse, L., Sainte-Beuve, J., and Bonfils, F. Investigating natural rubber composition with Fourier Transform Infrared (FT-IR) spectroscopy: A rapid and non-destructive method to determine both protein and lipid contents simultaneously. Polymer Testing 43 (2015): 83-93.
- [31] Gopalakrishnan, J. and Kutty, S.K.N. Mechanical, thermal, and rheological properties of dynamically vulcanized natural rubber-toughened polystyrene. Elastomers and plastics 47 (2013): 153-169.
- [32] Ho, C.C. and Khew, M.C. Low glass transition temperature (T_g) rubber latex film formation studied by atomic force microscopy. Langmuir 16 (2000): 2436-2449.

- [33] Minh, Q.T., Hiroshi, M., Naogutsu, N., Yuki, W., Fumio, Y., and Masao, T. Properties of crosslinked polylactides (PLLA & PDLA) by radiation and its biodegradability. European Polymer Journal 43 (2007): 1779-1785.





APPENDICES

จุฬาลงกรณ์มหาวิทยาลัย
CHULALONGKORN UNIVERSITY

APPENDIX A

Thermal properties

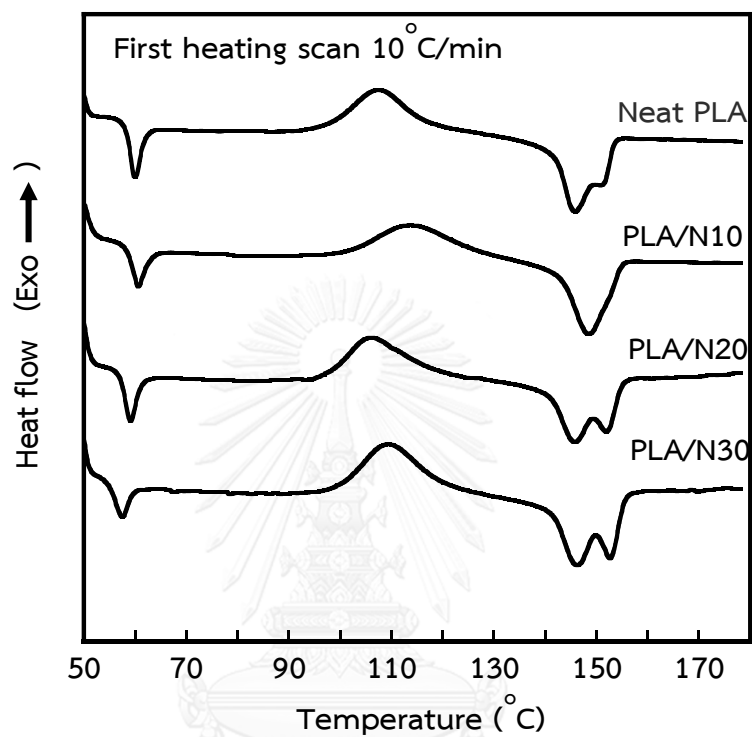


Figure A.1 DSC thermograms in the first heating scan of PLA/NRL films

Table A.1 Thermal properties of PLA/NRL films in the first heating scan

Samples	$T_{g\text{ PLA}}$ (°C)	T_{cc} (°C)	T_{m1} (°C)	T_{m2} (°C)	ΔH_{cc} (J/g)	ΔH_m (J/g)	% X_c
Neat PLA	57.4	107.6	145.8	151.47	22.99	25.99	3.23
PLA/N10	57.9	114.0	148.6		18.48	24.53	7.23
PLA/N20	56.3	105.4	145.0	152.0	23.53	26.2	3.59
PLA/N30	55.4	109.5	146.3	152.8	21.27	24.59	5.10

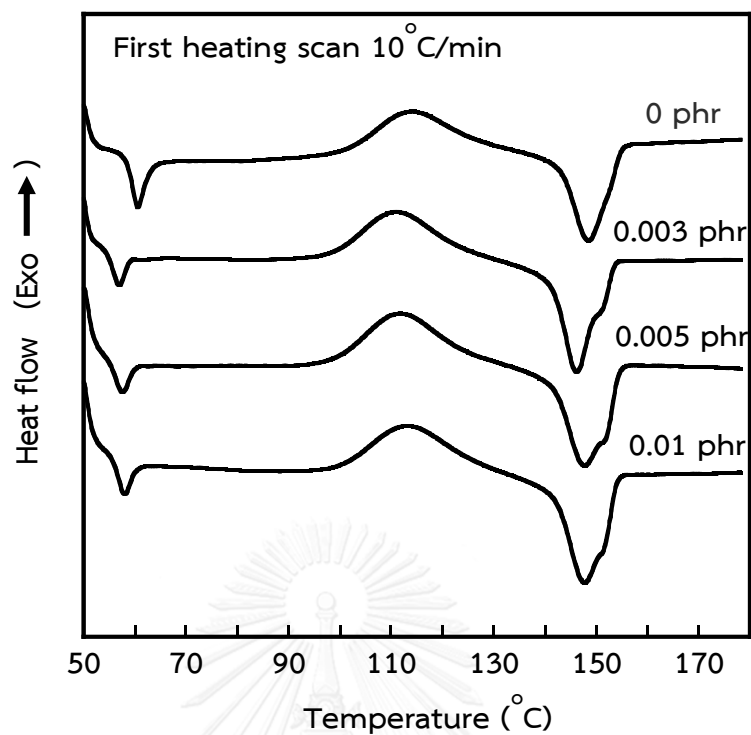


Figure A.2 DSC thermograms in the first heating scan of PLA/N10/DCP films

Table A.2 Thermal properties of PLA/NRL films in the first heating scan

DCP content (phr)	$T_{g\text{ PLA}}$ (°C)	T_{cc} (°C)	T_{m1} (°C)	T_{m2} (°C)	ΔH_{cc} (J/g)	ΔH_m (J/g)	$\%X_c$
0	58.0	114.0	148.6		18.48	24.53	7.23
0.003	51.9	112.8	146.2	151.4	20.09	24.43	5.19
0.005	52.7	110.7	147.6	152.1	20.23	24.81	5.47
0.01	53.8	111.7	147.9	151.9	20.06	24.50	5.30

APPENDIX B

Mechanical properties

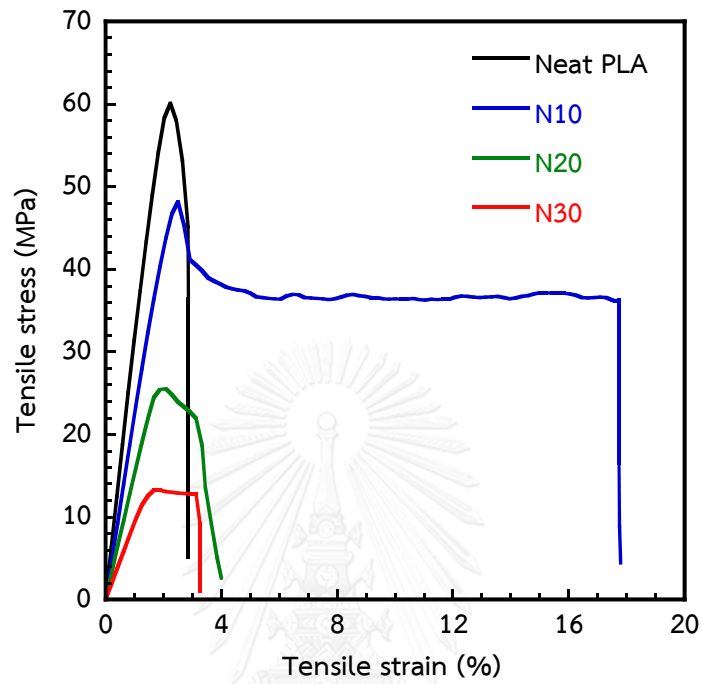


Figure B.1 Stress strain curve of PLA/NRL blend films

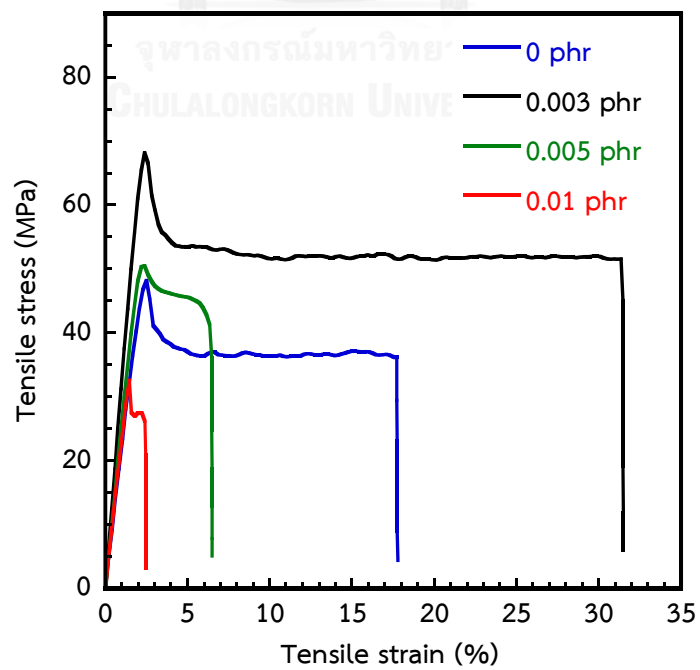


Figure B.2 Stress strain curve of PLA/N10 with DCP content of 0.003, 0.005 and 0.01 phr

Table B.1 Tensile properties in MD of PLA films

No.	Tensile strength (MPa)	Young's Modulus (MPa)	Elongation at break (%)	Tensile toughness (mJ)
1	55.05	3194.93	1.88	27.64
2	54.08	3275.71	2.14	33.53
3	52.92	3030.61	2.19	32.28
4	53.38	2927.92	2.40	38.90
5	52.87	3112.78	2.01	30.26
Avg	53.66	3108.39	2.12	32.52
S.D.	0.92	136.13	0.19	4.20

Table B.2 Tensile properties in MD of PLA/N10 films

No.	Tensile strength (MPa)	Young's Modulus (MPa)	Elongation at break (%)	Tensile toughness (mJ)
1	25.54	2073.80	13.65	117.15
2	24.25	1980.20	20.56	169.37
3	20.88	1930.80	15.24	115.99
4	24.10	1998.80	13.33	112.84
5	20.55	1943.10	18.72	135.40
Avg	23.06	1985.34	16.30	130.15
S.D.	2.22	56.55	3.20	23.64

Table B.3 Tensile properties in MD of PLA/N20 films

No.	Tensile strength (MPa)	Young's Modulus (MPa)	Elongation at break (%)	Tensile toughness (mJ)
1	15.67	1245.00	4.29	22.31
2	19.28	1326.00	3.30	21.97
3	18.39	1291.50	3.56	24.30
4	18.02	1273.80	2.95	18.12
5	19.60	1250.30	3.59	26.88
Avg	18.19	1277.32	3.54	22.72
S.D.	1.55	33.01	0.50	3.23

Table B.4 Tensile properties in MD of PLA/N30 films

No.	Tensile strength (MPa)	Young's Modulus (MPa)	Elongation at break (%)	Tensile toughness (mJ)
1	11.19	849.92	2.16	13.38
2	10.97	841.99	2.40	14.93
3	12.20	861.20	2.26	15.15
4	11.97	868.43	2.03	12.58
5	11.99	844.82	2.07	13.37
Avg	11.66	853.27	2.18	13.88
S.D.	0.55	11.21	0.15	1.11

Table B.5 Tensile properties in MD of PLA/N10 films blended with 0.003 phr of DCP

No.	Tensile strength (MPa)	Young's Modulus (MPa)	Elongation at break (%)	Tensile toughness (mJ)
1	39.55	2872.86	30.03	395.01
2	40.36	2869.91	24.47	328.71
3	44.92	2919.39	22.49	333.34
4	41.82	2923.15	20.99	315.05
5	40.84	2903.19	25.27	358.32
Avg	41.50	2897.70	24.65	346.09
S.D.	2.08	25.19	3.44	31.51

Table B.6 Tensile properties in MD of PLA/N10 films blended with 0.005 phr of DCP

No.	Tensile strength (MPa)	Young's Modulus (MPa)	Elongation at break (%)	Tensile toughness (mJ)
1	35.00	2287.20	4.67	57.21
2	34.46	2196.70	3.51	41.63
3	31.38	2229.10	3.73	42.93
4	32.92	2160.70	5.03	59.89
5	31.80	2282.00	5.02	61.96
Avg	33.11	2231.14	4.39	52.72
S.D.	1.59	54.50	0.72	9.69

Table B.7 Tensile properties in MD of PLA/N10 films blended with 0.01 phr of DCP

No.	Tensile strength (MPa)	Young's Modulus (MPa)	Elongation at break (%)	Tensile toughness (mJ)
1	31.94	2248.30	3.73	43.86
2	32.92	2279.60	3.35	38.48
3	29.23	2149.00	3.45	39.15
4	33.92	2130.40	2.77	30.87
5	32.38	2299.70	4.05	49.32
Avg	32.08	2221.40	3.47	40.34
S.D.	1.76	77.08	0.48	6.85

Table B.8 Tensile properties in TD of Neat PLA films

No.	Tensile strength (MPa)	Young's Modulus (MPa)	Elongation at break (%)	Tensile toughness (mJ)
1	71.72	3046.14	3.04	65.44
2	73.29	3109.78	2.99	66.80
3	73.61	3196.18	3.11	70.97
4	70.01	3136.43	2.84	55.80
5	78.34	3285.26	3.09	71.26
Avg	73.39	3154.76	3.01	66.05
S.D.	3.12	90.70	0.11	6.27

Table B.9 Tensile properties in TD of PLA/N10 films

No.	Tensile strength (MPa)	Young's Modulus (MPa)	Elongation at break (%)	Tensile toughness (mJ)
1	45.16	1982.33	13.48	202.09
2	37.28	1839.64	20.40	253.77
3	41.37	1893.99	15.69	207.84
4	58.92	2506.08	14.43	247.05
5	48.19	2155.82	18.53	264.21
Avg	46.18	2075.57	16.50	234.99
S.D.	8.21	268.84	2.89	28.16

Table B.10 Tensile properties in TD of PLA/N20 films

No.	Tensile strength (MPa)	Young's Modulus (MPa)	Elongation at break (%)	Tensile toughness (mJ)
1	25.55	1521.80	4.00	33.30
2	28.32	1544.70	3.38	31.96
3	26.17	1525.70	4.19	31.11
4	28.06	1525.70	4.90	33.40
5	25.96	1523.40	3.89	35.47
Avg	26.81	1528.26	4.07	33.05
S.D.	1.28	9.34	0.55	1.66

Table B.11 Tensile properties in TD of PLA/N30 films

No.	Tensile strength (MPa)	Young's Modulus (MPa)	Elongation at break (%)	Tensile toughness (mJ)
1	12.50	929.19	3.26	25.44
2	11.76	922.76	3.44	25.91
3	12.34	884.85	3.75	28.91
4	13.22	920.33	3.26	26.33
5	15.29	878.46	3.08	27.85
Avg	13.02	907.12	3.36	26.89
S.D.	1.37	23.58	0.25	1.45

Table B.12 Tensile properties in TD of PLA/N10 films blended with 0.003 phr of DCP

No.	Tensile strength (MPa)	Young's Modulus (MPa)	Elongation at break (%)	Tensile toughness (mJ)
1	55.81	2630.50	40.97	654.21
2	64.31	2935.56	27.36	514.59
3	68.22	3212.36	31.49	646.13
4	59.13	3029.26	29.69	588.63
5	64.62	3091.14	35.18	691.64
Avg	62.42	2979.76	32.94	619.04
S.D.	4.91	219.60	5.32	69.06

Table B.13 Tensile properties in TD of PLA/N10 films blended with 0.005 phr of DCP

No.	Tensile strength (MPa)	Young's Modulus (MPa)	Elongation at break (%)	Tensile toughness (mJ)
1	50.50	2532.12	6.47	128.48
2	52.97	2589.62	8.82	191.36
3	49.28	2270.85	6.00	107.86
4	45.45	2207.24	6.09	107.57
5	45.24	2177.56	7.43	122.38
Avg	48.69	2355.48	6.96	131.53
S.D.	3.33	191.58	1.18	34.67

Table B.14 Tensile properties in TD of PLA/N10 films blended with 0.01 phr of DCP

No.	Tensile strength (MPa)	Young's Modulus (MPa)	Elongation at break (%)	Tensile toughness (mJ)
1	49.47	2397.09	4.17	74.16
2	47.38	2371.93	4.45	79.07
3	42.84	2378.46	4.61	72.32
4	49.47	2204.78	3.33	50.71
5	46.19	2314.78	2.6	37.47
Avg	47.07	2333.41	3.83	62.75
S.D.	2.75	78.20	0.85	17.83

Table B.15 Impact strength of PLA/NRL films

Impact strength (J/cm)	Neat PLA	PLA/N10	PLA/N20	PLA/N30
1	2.64	3.31	1.07	1.15
2	2.64	3.31	1.07	1.15
3	2.64	3.31	1.59	1.18
4	3.16	3.31	1.59	1.18
5	3.16	3.31	1.59	2.06
Avg	2.85	3.31	1.38	1.35
S.D.	0.28	0.00	0.28	0.40

Table B.16 Impact strength of PLA/N10/DCP

Impact strength (J/cm)	PLA/N10/DCP at DCP content of (phr)			
	0	0.003	0.005	0.01
1	3.31	7.30	5.92	5.32
2	3.31	7.67	5.92	4.67
3	3.31	7.67	5.92	4.67
4	3.31	7.67	6.66	4.67
5	3.31	7.06	6.00	4.67
Avg	3.31	7.47	6.08	4.80
S.D.	0.00	0.28	0.32	0.29

Table B.17 Tear strength of PLA/NRL

samples	Tear strength (Nm)	
	MD	TD
Neat PLA	342.5±0.00	456.5±0.00
PLA/N10	285.5±0.00	326.2±0.00
PLA/N20	114.2±0.00	228.4±0.00
PLA/N30	63.46±0.00	67.19±0.00

Table B.18 Tear strength of PLA/N10/DCP

PLA/N10/DCP at DCP content of (phr)	Tear strength (Nm)	
	MD	TD
0	285.5±0.00	326.2±0.00
0.003	380.5±0.00	407.7±0.00
0.005	329.3±0.00	342.5±0.00
0.01	323.1±0.00	335.7±0.00

APPENDIX C

Oxygen and water permeation

Table C.1 Water permeation of PLA/NRL films

No.	Water vapor permeation (gm.mil/m ² .day.atm)			
	Neat PLA	PLA/N10	PLA/N20	PLA/N30
1	177.874	256.99	276.53	324.66
2	162.65	245.00	286.94	348.24
3	172.13	260.00	286.32	324.97
Avg	170.88	254.00	283.26	332.62
S.D.	7.69	7.94	5.84	13.53

Table C.2 Water permeation of PLA/N10/DCP films

No.	Water vapor permeation (gm.mil/m ² .day.atm)			
	DCP content of (phr)			
	0	0.003	0.005	0.01
1	256.99	212.54	226.90	233.80
2	245.00	209.32	223.63	237.75
3	260.00	208.64	221.83	239.30
Avg	254.00	210.17	224.12	236.95
S.D.	7.94	2.09	2.57	2.84

Table C.3 Oxygen permeation of PLA/NRL films

No.	Oxygen permeation (cc.mil/m ² .day.atm)			
	Neat PLA	PLA/N10	PLA/N20	PLA/N30
1	565.48	1119.78	1263.63	1281.69
2	561.57	1105.90	1235.43	1264.36
3	599.12	1155.62	1314.92	1378.74
Avg	575.39	1127.10	1271.33	1308.26
S.D.	20.64	25.66	40.30	61.65

Table C.4 Oxygen permeation of PLA/N10/DCP films

No.	Oxygen permeation (cc.mil/m ² .day.atm)			
	PLA/N10/DCP at DCP content of (phr)			
	0	0.003	0.005	0.01
1	1119.78	717.62	770.63	799.21
2	1105.90	720.01	780.63	797.72
3	1155.62	705.46	775.46	792.73
Avg	1127.10	714.37	775.57	796.55
S.D.	25.66	7.80	5.00	3.39

APPENDIX D

The size distribution of rubber domain

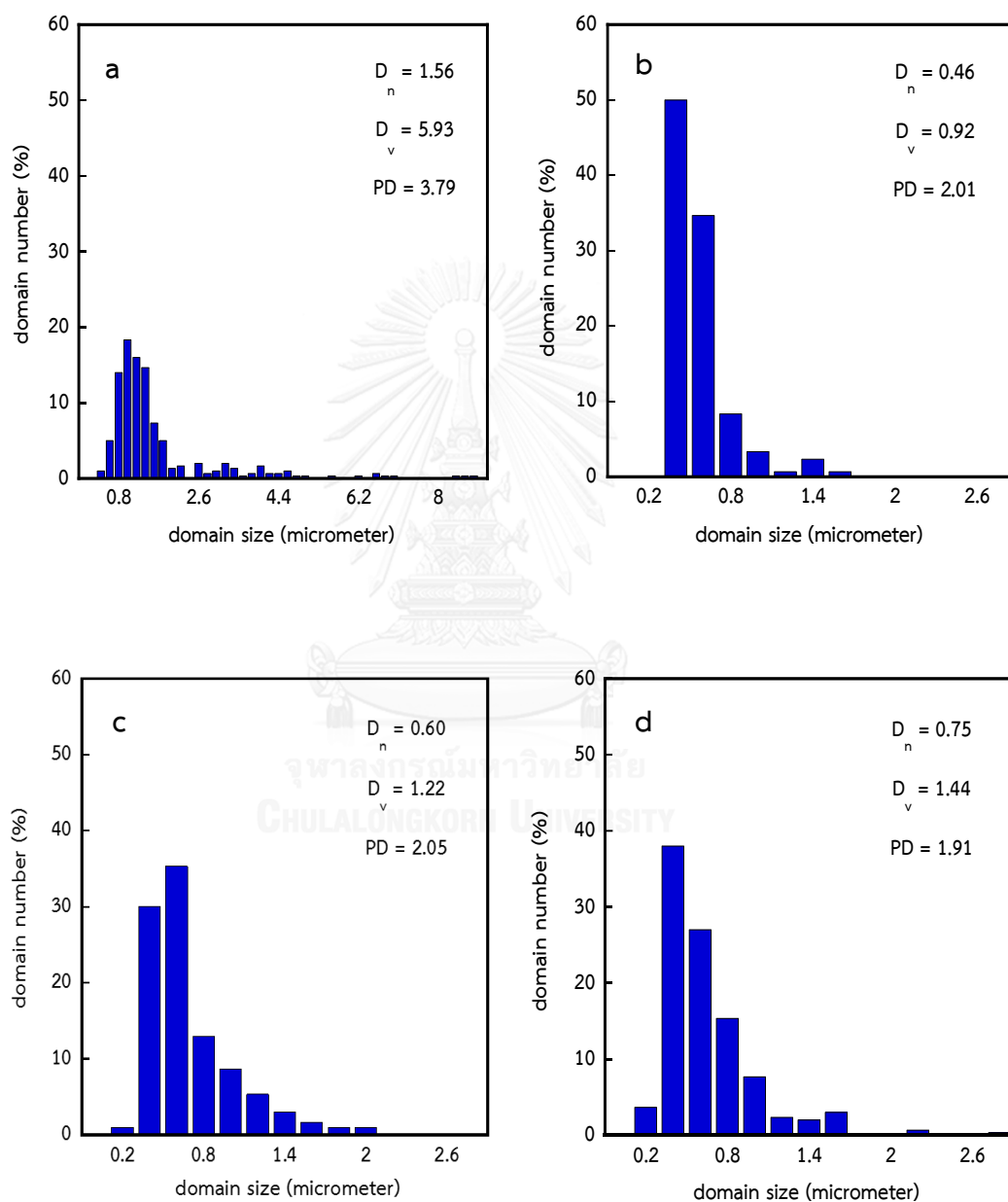


Figure D.1 Size distribution of NR domain in the PLA/N10/DCP films for different DCP

content a) 0 phr, b) 0.003 phr, c) 0.005 phr and d) 0.01 phr

VITA

Ms. Parichat Pratumpol was born on February 20, 1990 in Khonkaen, Thailand. She finished high school at Khonkaen Wittayayon School, Khonkaen. In 2013, she received the Bachelor's Degree from Department of Chemical Engineering, Faculty of Engineering, King Mongkut's University of Technology, Thonburi. She continued her study for Master's Degree in Chemical Engineering at the Department of Chemical Engineering, Faculty of Engineering, Chulalongkorn University in June, 2013.

She was invited for poster presentation in the title of "Improvement of mechanical properties of poly(lactic acid) blown films by incorporation with natural rubber latex", During March 23-24, 2015 at the 1st Rajamangala University of Technology Lanna Chiangrai Conference 2015 in Chiangrai, Thailand.

